UNIVERSITÄTSKLINIKUM HAMBURG-EPPENDORF

Zentrum für Experimentelle Medizin,

Institut für Biochemie und Molekulare Zellbiologie

Institutsdirektor: Prof. Dr. rer. nat. Dr. med. habil. Andreas H. Guse

Stellvertretender Institutsdirektor: Prof. Dr. rer. nat. Jörg Heeren

Role of P2X7 receptor in adipose tissue function

Dissertation

Zur Erlangung des Grades eines Doktors der Medizin/Zahnmedizin

an der Medizinischen Fakultät der Universität Hamburg

Vorgelegt von:

Tian Tian

aus Anhui (China)

Hamburg 2019

(wird von der Medizinischen Fakultät ausgefüllt)

Angenommen von der

Medizinischen Fakultät der Universität Hamburg am: 08.10.2019

Veröffentlicht mit Genehmigung der

Medizinischen Fakultät der Universität Hamburg.

Prüfungsausschuss, der/die Vorsitzende: Prof. Dr. Jörg Heeren

Prüfungsausschuss, zweite/r Gutachter/in: Prof. Dr. Friedrich Nolte

Contents

1. HYPOTHESIS

Adipose tissue is a complex organ with endocrine, metabolic, and immune regulatory roles. Several studies show that obesity is associated with chronic subclinical inflammation in white adipose tissue (WAT) depots. Recent studies suggest that extracellular adenosine nucleotides (ANs) regulate metabolic and differentiation processes in WAT and brown adipose tissue (BAT) via the purinergic signaling network which is composed of ANs, ecto-enzymes, and purinergic receptors. However, the precise roles of secreted ANs regulating adipose metabolism and intercellular communication under physiological and pathophysiological conditions remain largely unknown. Among purinergic receptors, P2X7 receptor has received special attention because of association of human P2X7 single nucleotide polymorphism (SNPs) to various inflammatory pathways.

The hypothesis of the thesis project is that the intercellular crosstalk between adipocytes, endothelial cells, and tissue-resident immune cells within BAT and WAT is regulated, at least in part, by extracellular AN. In the current project, I want to decipher the functional relevance of proteins especially P2X7 regulating extracellular ANs levels for metabolic inflammation and energy combustion in WAT and BAT.

2. INTRODUCTION

2.1 Adipose Tissue

Currently adipose tissue is regarded as a complex organ with metabolic, endocrine, and immune regulatory functions. Mammalians have two types of adipose tissue: white adipose tissue (WAT) and brown adipose tissue (BAT). WAT, which is mainly composed of white adipocytes, stores energy in the form of triglycerides. BAT is primarily composed by brown adipocytes and utilizes fat and glucose to produce heat through uncoupling mitochondrial oxidative phosphorylation. The balance between the two types of adipose tissue contributes to the maintenance of energy homeostasis. In recent years, adipose tissue has been recognized as a major endocrinologically active organ that produces and secrets bioactive factors such as leptin, resistin, cytokines, and several complement components (Kershaw and Flier, 2004). Besides adipocytes, adipose tissue contains the stromal vascular fraction (SVF) cells including fibroblasts, preadipocytes, endothelial cells and a variety of immune cells such as macrophages, T cells, and B cells.

2.1.1 Characteristics of adipose tissue

Adipocytes, which are also called fat cells or adipose cells, are the predominant cell type of adipose tissue. According to their different original, morphological and functional features, adipocytes can be classified into three types: white adipocyte, brown adipocyte and beige adipocyte. A white adipocyte is a kind of spherical unilocular cell, which contains a single large lipid droplet and a peripheral located nucleus in the cytoplasm. The size of white adipocyte largely depends on the lipid content stored in it. In mature white adipocyte, the single lipid droplet, which consists of triglycerides, occupies more than 90% of cell volume. In contrast to unilocular white adipocyte, the brown adipocyte is multilocular fat cell with a number of small vacuoles containing lipid in cytoplasm. Brown adipocytes are characterized by abundant mitochondria carrying uncoupling protein-1 (UCP-1) in the inner mitochondrial membrane, which is a unique protein and

often regarded as the defining marker of BAT because of its ability to disconnect oxidative phosphorylation from ATP synthesis (Figure1). Besides the two classical types of adipocytes, a kind of UCP-1 expressing adipocytes in WAT is classified as the third type: beige adipocyte (or brown in white: brite adipocyte), which is similar to brown adipocyte in morphology and its capacity to do adaptive thermogenesis(Rosen and Spiegelman, 2014)(Himms-Hagen, 1995)(Cinti, 2001)(Lidell et al., 2013)(Bartelt and Heeren, 2014)
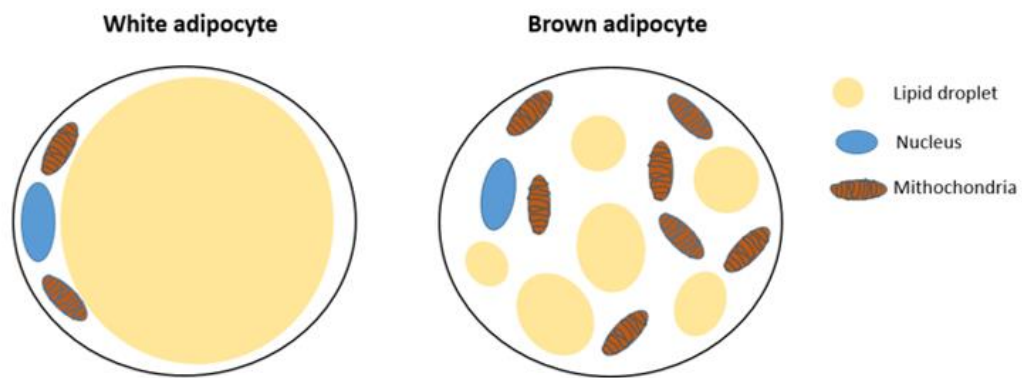
Figure1. Adipocyte structure. *A single large lipid droplet occupies most of the space within white adipocyte and nucleus and other cell organelles are pushed towards the edges of the cell which is bounded by the plasma membrane. Brown adipocyte is characterized by multiple small lipid droplets and a high density of mitochondria.*

White fat can be found in most species, but its distribution varies in different species. In human beings, WAT can be found all around the body, and there are two main locations of WAT: inside the abdomen, where the largest fat deposits surround inner organs including the momentum, the intestine and the peritoneal region, while in the subcutaneous layer, WAT distributes mostly in the hypodermis of buttocks, thighs and abdomen (Wronska and Kmiec, 2012). Besides these major deposits, smaller WAT are also located in other areas of the body, including epicardial, perivascular, periarticular, intramuscular, and bone marrow deposits (Iozzo, 2011).

Unlike WAT, BAT is an organ which exists only in mammals. It has been believed for long time that active BAT depot can only be found in infants and young children and decreases rapidly with aging (Lean, 1989; Nuutila, 2015). However, ~10 years ago with the use of ^{18}F-fluorodeoxyglucose (FDG) to observe tumor metastasis in positron emission tomography (PET), Jan Nedergaard, et al, found FDG uptake in brown fat, indicating the presence of functionally active BAT in adults (Nedergaard et al., 2007). Brown fat in human beings can be divided anatomically as visceral BAT, which includes perivascular BAT, periviscus BAT and BAT which is around solid organs, and subcutaneous BAT, where the depots locate mostly between anterior neck muscles and supraclavicular fossa, under the clavicles, in the axilla, in the anterior abdominal wall and in the inguinal area (Sacks and Symonds, 2013). By calculating the maximal standard uptake values (SUV max) of the FDG, it is demonstrated that in humans metabolically active BAT is relatively abundant in the neck and upper-chest regions (Frontini and Cinti, 2010).

2.1.2 Functions of adipose tissue

2.1.2.1 Adipogenesis

Adiposity is closely related to both increase in adipocyte size (hypertrophy) and number (hyperplasia). Understanding the process of adipocyte formation, called adipogenesis, is vital to fight against worldwide obesity epidemic. Adipogenesis is the process of cell differentiation during which mesenchymal stem cells (MSCs) develop into adipocytes and involves mainly two phases. In the first phase, also known as adipocyte determination, pluripotent stem cells are converted into preadipocytes, and the second phase involves terminal differentiation of preadipocytes into mature adipocytes (Ali et al., 2013; Farmer, 2006; Lefterova and Lazar, 2009a).

Adipogenesis is regulated by complex network of numerous transcription factors and their products including proteins which are important for adipocyte development and function. During the last several years, the transcriptional control of adipogenesis has

been intensively studied. Among these transcription factors peroxisome proliferator-activated receptor gamma (PPAR-γ) functions as the master regulator of adipogenesis in all types of adipose tissue, without which no precursor cells have been identified being capable of adipocyte differentiation (Rosen et al., 1999, 2002). PPAR-γ belongs to the nuclear receptor family of ligand-activated transcription factors and is expressed as two isoforms PPAR-γ1 and PPAR-γ2. PPAR-γ1 is expressed in many tissues and abundant in adipocytes, whereas PPAR-γ2 is almost specifically expressed in adipose (Vidal-Puig et al., 1996). PPAR-γ regulates various gene transcriptions by binding to DNA with its heterodimeric partner retinoid X receptors (RXR) (Tontonoz et al., 1994a, 1994b). CCAAT/enhancer-binding proteins (C/EBPs) is also one of the first transcription factors identified to be involved in adipocyte differentiation. C/EBPs belong to a family of transcription factors composed of six members, named from C/EBPα to C/EBPζ. Along with PPAR-γ, C/EBPs are crucial for transcriptional regulation during adipogenesis. In the early stage, C/EBPβ and -d activate expression of PPARγ, C/EBPα and other genes which are related to adipogenesis. PPARr binds to downstream genes with C/EBPα and β frequently occupying C/EBP-response elements nearby. Furthermore there is evidence showing that PPARr share 30–60% of binding sites with C/EBPs (Schmidt et al., 2011). However, the overlap of PPAR-γ and C/EBPs are still unclear and the cooperation of PPAR-γ between C/EBPs remains to be explored. Other factors such as Kruppel-like transcription factors (KLFs), Wingless and INT-1 proteins (Wnts), signal transducer and activator of transcription, anti-adipogenic factors such as GATA transcription factors, early B cell factor, and interferon signaling also play important roles in regulating adipogenesis (Lefterova and Lazar, 2009b)

2.1.2.2 Lipogenesis and lipolysis

Adipose tissue is a metabolic organ which stores and mobilizes lipid through the process of lipogenesis and lipolysis, respectively.

De novo lipogenesis (DNL), which is also called synthesis of fatty acids endogenously, encompasses both *de novo* fatty acids synthesis and triglyceride (TG) synthesis. During fatty acids synthesis, acetyl-coenzyme A (acetyl-CoA) derived from glucose and other carbon precursors is converted into fatty acids in the presence of NADPH. Acetyl-CoA carboxylase (ACC) and fatty acid synthase (FAS) are two key enzymes that regulate biosynthesis of fatty acids. In normal biology, liver and adipose tissue are the major organs where fatty acids synthesis take place. However, due to the relatively lower activation of fatty acids biosynthesis in adipose tissue compared to liver, adipocytes use free fatty acids which are mainly from circulating TG in very low-density lipoproteins (VLDL) and chylomicrons (Kersten, 2001). Lipoprotein lipase (LPL) is the central enzyme which hydrolyzes TG in lipoproteins into free fatty acids (FFAs) and facilitates entry of FFAs into adipocytes (Kersten, 2014). In the endoplasmic reticulum of adipocytes, FFAs are esterified to glycerol, which is another important metabolite from glucose, to synthesize TG. There are two master transcriptional regulators of lipogenesis, sterol regulatory element-binding protein 1c (SREBP1c) and carbohydrate response element-binding protein (ChREBP) (Eissing et al., 2013; Ferre and Foufelle, 2007), regulating expression of key lipogenic genes. Insulin plays an important role in fatty acids uptake and esterification through many mechanisms including control of ACC and LPL activity, promoting uptake of glucose by adipocytes, stimulating expression of transcriptional regulators (Dimitriadis et al., 2011; Picard et al., 1999).

In contrast to lipogenesis which converts excess carbohydrates into lipids for storage, lipolysis is the process in which TG is hydrolyzed into fatty acids and glycerol (Bolsoni-Lopes and Alonso-Vale, 2015). Lipolysis consists of sequential steps: in the first step, which is catalyzed by adipocyte triglyceride lipase (ATGL), TG is hydrolyzed into diacylglycerol and one non-esterified fatty acid. After that, hormone-sensitive lipase (HSL) catalyzes the hydrolysis of diacylglycerol into monoacylglycerol and a second fatty acid. Finally, monoglyceride lipase (MGL) efficiently cleaves monoacylglycerol into glycerol and the last fatty acid (Lass et al., 2011).

Lipogenesis is induced upon increased energy demand during fasting and exercise, supplying metabolite glycerol for gluconeogenesis and fatty acids for oxidation. Peroxisome proliferator-activated receptor (PPARS) and 5' AMP-activated protein kinase (AMPK) are important molecules in regulating lipolysis and lipid metabolism (Zechner et al., 2009). Meanwhile, norepinephrine (NE) released by the sympathetic nervous system (SNS) mediates lipolysis by stimulating β-adrenoceptor and regulating hormone sensitive lipase and perilipin A phosphorylation (Bartness et al., 2014). In summary, the balance between lipogenesis and lipolysis plays a critical role in lipid and energy homeostasis.

2.1.2.3 Thermogenic function

Thermogenesis, literately defined as the process of heat production, is a primary effector of thermoregulation. To maintain relatively stable core body temperature in response to changes of environmental temperature and metabolic conditions, homoeothermic animals can produce endogenous body heat through thermogenesis (Morrison, 2016; Tansey and Johnson, 2015).

Depending on whether associated with the muscle activity of shivering or not, thermogenesis can be classified as shivering and non-shivering thermogenesis. Shivering is considered to play a major role in defending body temperature following acute exposure to cold, while during prolonged cold exposure classical non-shivering thermogenesis is the main response towards increased heat loss (Griggio, 1982).

Non-shivering thermogenesis is a process which is fully dependent on brown and beige adipocytes. Cold stimulates the sympathetic nervous system, releasing norepinephrine (NE) which binds to β3-adrenoceptor on cell surface of these thermogenic adipocytes. This binding activates intracellular signaling cascades including cAMP/protein kinase A (PKA) pathway, resulting in lipolysis on lipid droplets, and the released FFAs interact with UCP-1 on mitochondria membrane, leading to respiration in the mitochondria and consequently heat generation (Cannon and Nedergaard, 2011). In addition to non-shivering thermogenesis, brown fat also plays an important role in diet-induced

thermogenesis (Rothwell and Stock, 1997). Chronically increased food intake will develop obesity, leading to upregulated leptin signaling to the regulatory center in the brain which can activate BAT (Cannon, 2004; Commins et al., 2001). UCP-1 ablation can entirely inhibit leptin from activating BAT in mice (Feldmann et al., 2009).

In white fat depots, beige/brite adipocytes can be activated by prolonged cold exposure and adrenergic stimulation with remarkable increase in UCP-1 expression (Cousin et al., 1992; Nedergaard and Cannon, 2014; Petrovic et al., 2010; Young et al., 1984). Until now, many regulatory pathways are thought to be involved in this so-called "browning" process, such as PGC-1α, C/EBPα, PPARγ, PRDM16, SRC-1 and transcription factors include FoxC2, (forkhead box protein C2), IRISIN (secreted protein), BMP7 (bone morphogenetic protein 7) and Fibroblast growth factor 21 (FGF21) (Brychta and Chen, 2017; Jeremic et al., 2017; Lodhi et al., 2013).

2.1.2.4 Endocrine function

Adipose tissue is an endocrine active organ producing a variety of hormones which is critical for regulation of systemic metabolism and inflammation. Adipocyte-derived factors, which are called adipokines, have been extensively studied in the recent years. Leptin is the firstly discovered adipokine and encoded by the obesity (ob) gene. By binding to its specific receptor in the hypothalamus, leptin can decrease food intake and regulate fat metabolism (Zhang et al., 1994). Adiponectin, which is the second adipokine to be found, can bind to its receptors (AdipoR1 and AdipoR2) distributed in multiple tissues, regulating insulin sensitivity (Hoffstedt et al., 2004; Hui et al., 2012; Tomas et al., 2002). In liver, adiponectin suppresses gluconeogenesis through various downstream signaling pathways, such as AMPK, ceramide, Ca^{2+} and PPARα (Combs et al., 2004) Another important function of adiponectin is regulating thermogenesis and energy homeostasis (Hui et al., 2015; Masaki et al., 2003). Other adipokines includes resistin, chemerin, apelin, visfatin, plasminogen activator inhibitor 1(PAI1), monocyte chemoattractant protein 1 (MCP1), tumor necrosis factor alpha (TNFα), and interleukin (Fasshauer and Bluher, 2015). However, adipose-resident immune cells and endothelial

cells can also secret hormones, such as apelin, PAI1, MCP1, TNFα, and IL6 contributing to both the endocrine and metabolic function of adipose tissue (Boucher et al., 2005; Kanda et al., 2006; Weisberg et al., 2003).

2.2 Purinergic signaling

Nucleosides and nucleotides are involved in many important functions in physiology and pathophysiology via an extracellular purinergic signaling network, which consists of ectoenzymes hydrolyzing ATP to adenosine, purinergic receptors and transporters (Tozzi and Novak, 2017). In adipose tissue, extracellular adenosine 5'-triphosphate (ATP) is mainly released from presynaptic neural cells of sympathetic nerves and functions as a classical neurotransmitter. The hydrolysis of extracellular ATP to adenosine consists of sequential steps and catalyzed by cell-surface located metabolizing enzymes, which are also called ectoenzymes and ecto-nucleotidases and have widespread distributions in the body. There are four major subfamilies of nucleotidases: ectonucleoside triphosphate diphosphohydrolases (E-NTPDases)/CD39, ecto-5'-nucleotidase (eN)/CD73, ecto-nucleotide pyrophosphatase/phosphodiesterases (E-NPPs), and alkaline phosphatases (APs). Among these enzymes CD39 and CD73 have been studied extensively (Burnstock, 2014; Zimmermann et al., 2012). CD39 is a rate-limiting ectoenzyme that hydrolyzes ATP/ADP to AMP, while CD73 is responsible for the degradation of AMP to adenosine. Thus, the enzymatic activities of CD39 and CD73 play crucial roles in duration, and magnitude of purinergic signals (Zhao et al., 2017).

Currently purinergic receptors, which are also called purinoceptors, are sub-classified as P1, P2X and P2Y receptors according to their different activation mechanisms. P1 receptors are adenosine receptors (ARs) and have four distinct subtypes, i.e., A1, A2A, A2B, and A3 receptor, which are all typical G-protein-coupled receptors (GPCRs). Each of them has unique tissue distribution and can be activated or inhibited by specific agonists or antagonists, respectively (Burnstock, 2006; Jacobson and Gao, 2006).

P2Y receptors are also members of G-protein-coupled receptor family, which can be

activated by a range of purine and pyrimidine mono- and -dinucleotides. Eight subtypes of P2Y receptors have been cloned in humans: P2Y1, P2Y2, P2Y4, P2Y6, P2Y11, P2Y12, P2Y13, and P2Y14 (the missing numbers represent in other non-mammalian animals). The ARs and P2Ys share the similar structure of GPCR class A family, consisting of seven transmembrane α-helices (TM) connected by three extracellular loops and three intracellular loops, an extracellular N-terminus and an intracellular C-terminus (Fredriksson, 2003; Jacobson et al., 2012). Unlike ARs and P2Ys, P2X receptors are ligand-gated ion channel receptors and currently seven subtypes have been cloned, namely P2X1-7. P2Xs consist of two transmembrane domains (TM1 and TM2), intracellular N- and C-terminus, and extracellular loop which provides binding site for extracellular ATP (Figure 2) (North, 2016).

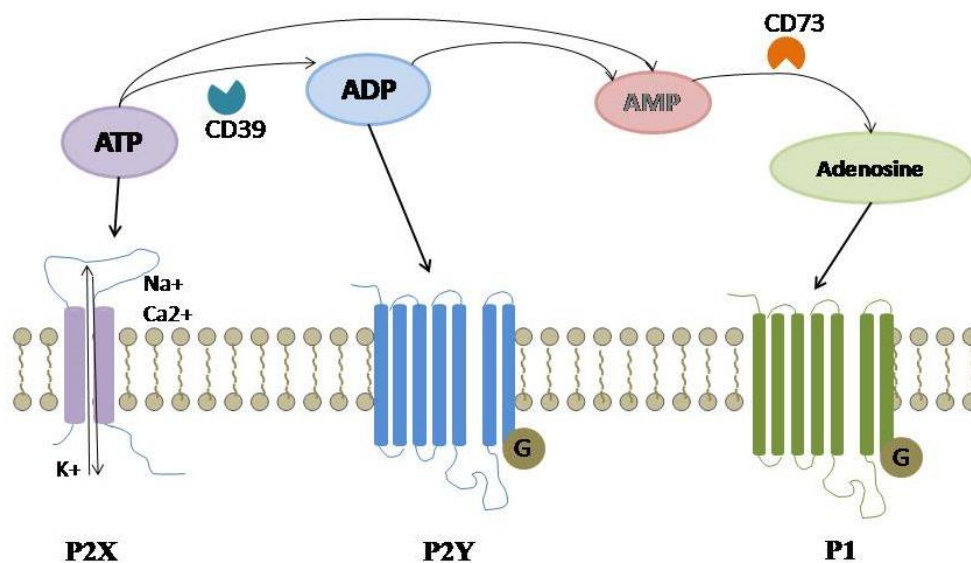**Figure 2.The autocrine/paracrine of purinergic signaling system**. *ATP can be released into extracellular compartment as eATP by stimulations including cellular stress, trauma, or agonist binding. Ectoenzymes located on the cell surface such as CD39 and CD73 can hydrolyze ATP to ADP, AMP and adenosine. P1 receptors specifically recognize adenosine while P2X and P2Y receptors bind to di- and tri-phosphate nucleotide*

molecules. P1 and P2Y receptors are G-protein-coupled receptors and P2X receptors are ligand-gated ion channels that are selective for Na+, K+, and Ca2+.

Extracellular adenosine is mainly generated from either the release of damaged cells or nucleotidase-mediated hydrolysis of ATP. To note recently few studies demonstrated that CD38 catalyzes the conversion of NAD^+ to adenosine through an alternative pathway (Horenstein et al., 2013). A1 and A3 receptors are coupled with G proteins of the Gi and Go family, leading to the inhibition of adenylyl cyclase activity. In contrast, A2A and A2B receptors are coupled with Gs or Gq proteins to activate adenylyl cyclase. Besides the classical adenylyl cyclase pathway, other pathways, such as phospholipase C (PLC), Ca^{2+} and mitogen-activated protein kinases (MAPKs), are also involved in adenosine signaling (Antonioli et al., 2013)

2.2.1 P1 and P2Y receptors

Extracellular adenosine level is variable, and can be regulated by several mechanisms, (i) the production of adenosine from precursor nucleotides, during which ectoenzymes play an essential role (ii) nucleoside transporters, which can transport adenosine across the membrane into cells, including concentrative nucleoside transporters (CNT1, CNT2, CNT3) and equilibrate nucleoside transporters (ENT1, ENT2, ENT3, and ENT4) (iii) adenosine deaminase (ADA1 and ADA2), which can convert adenosine into inosine (Rose and Coe, 2008).

Because of the complex system that controls extracellular adenosine signaling, it has been a challenge for many years to characterize functions of extracellular adenosine in pathological processes. By utilizing specific agonists, antagonists or inhibitors for different adenosine receptor subtypes, genetically deleting specific adenosine receptors or ectoenzymes (Generation, 1990), several breakthrough discoveries have been achieved. Many instances have revealed that adenosine signaling plays anti-inflammatory role in certain acute diseases status. Adenosine induced immunosuppressive effect is a negative regulator during neoplastic disease states for tumor growth and metastasis (Nelson and

Guyer, 2012) (Antonioli et al., 2013).

Human P2Y receptors can be divided into two subgroups according to sequence homology. The first subgroup includes P2Y1, 2, 4, 6, 11 subtypes and the second subgroup encompasses the P2Y12, 13, 14 subtypes. Some studies demonstrated that the two subgroups also couple with different G proteins: P2Y1, 2, 4, 6, and 11 bind to Gq/G11 while P2Y12, 13, 14 is coupled with Gi/0 proteins. ATP is the most abundant and the best-characterized endogenous ligand for P2Ys, and all P2Y subtypes except P2Y6R and P2Y14R can be activated by ATP. Other nucleotides, such as ADP, UTP, UDP and UDP-glucose are more specifically coupled with individual P2YRs. In response to binding to extracellular nucleotides P2Ys have conformational changes which activates G proteins, facilitating regulation of ion channels and intracellular signaling cascades, such as activating phospholipase C, release of intracellular calcium, altering adenylyl cyclase and cAMP levels (Burnstock, 2006). Mice with specific genetic deletion of P2YR subtypes (except of P2Y11, which is not expressed in mice) have been utilized to demonstrate functions of P2YRs, but only mild phenotypical alterations can be observed, revealing the potential redundancy or compensation mechanisms of P2YRs signaling.

2.2.2 P2X receptors

P2X receptors are ligand-gated-ion channels selective for Na^+, K^+, Ca^{2+}, that can be specifically activated by extracellular ATP. Seven P2X subtypes share common structure: two transmembrane domains (TM1 and TM2), intracellular N- and C- terminals, a large extracellular loop with an ATP binding site (Khakh and Alan North, 2006; Surprenant and North, 2009). Functional P2XRs are homotrimers or heterotrimers formed by three same or different subunits, with an ion-permeable channel pore in the middle of them. In response to binding of extracellular ATP to ATP binding site, ion channel conformational changes, resulting in the opening of the ion-permeable pore. Opening channel allows Na^+ and Ca^{2+} influx and K^+ efflux ,which leads to plasma membrane depolarization and

activation of various intracellular Ca^{2+} signaling processes, such as p38 MAPK or phospholipase A2 activation (Khakh and North, 2014). The channel opening time depends on the subunit makeup of the receptor.

P2XR family members have distinct functions. Among them, P2X7 receptors can induce a number of downstream events, including activation of nucleotide-binding oligomerization domain-like receptors (NLRs) mediated inflammasome, cell proliferation and death, metabolic events, and phagocytosis (Bartlett et al., 2014; Weber et al., 2010). P2X7 has been thought to locate only on cell surfaces of the hematopoietic cells, including macrophages, dendritic cells, monocytes, lymphocytes, osteoclasts, mast cells, etc. However, by using specific P2X7 antibodies, it is evident now that P2X7 present on membranes of many other cell types, such as fibroblasts, endothelial cells, and epithelial cells as well as in the central and peripheral nervous systems (Buell et al., 1998)(Adriouch et al., 2005)(Kurashima et al., 2012). Furthermore, recent studies also reveal the presence of P2X7 within intracellular space (Gu et al., 2000). Although P2X7 is known to have a widely distribution in mammalian body, it still remains largely unclear about the relative distribution of P2X7 in different cell types and tissues.

The gene encoding the P2X7 subunit is called P2rX7 which is found in over 50 species. In most species P2rX7 is demonstrated to comprise 13 exons but with different chromosomal localization. Human and mouse P2rX7 have ten (P2X7A–J) and four (P2X7a, P2X7k, P2X713b, and P2X713c) variants, respectively. Among them P2X7B have attracted special interests because it is widely expressed in many tissues in human beings. P2X7B is a shorter isoform with truncated C-terminal, and it retains the ability to form the channel pore but lacks the pore function (Adinolfi et al., 2010). Human P2rX7 is a highly polymorphic gene with a number of non-synonymous single-nucleotide polymorphisms (SNPs) which are identified to code protein sequences of extracellular domain and intracellular termini. Up to now, at least eight loss-of-function SNPs and three gain-of-function SNPs have been identified in human P2rX7. These SNPs are found to

influence P2X7 function and are associated with some disorders and diseases (Jørgensen et al., 2012).

P2X7 protein shares similar structure with other P2X receptors. Each monomeric subunit of P2X7 has a relatively a shorter amino termini and a longer intracellular carboxyl (C) termini which makes P2X7 subunit the largest in P2X family. The intracellular C-termini attracts interests because it contains multiple lipid and protein binding motifs, including SRC homology 3 (SH3)-binding domains, cytoskeleton binding domain and endotoxin (LPS)-binding region (Denlinger et al., 2001). Two transmembrane domains are connected by a large extracellular ATP-binding loop. On cell surface, functional P2X7 presents predominantly as homotrimeric receptors, with three extracellular domains interacting at several points and three second transmembrane domains locate centrally to form channel pore. P2X7 can also assembly heterotrimeric receptors with P2X4 and P2X3 receptors (together with protein sequence homology, P2rX7 and P2rX4 have close location on chromosome in mice and human) (Antonio et al., 2011; Boumechache et al., 2009).

P2X7 can be activated by extracellular ATP (or by nicotinamide adenine dinucleotide (NAD) in rodents) in the closed (apo) states. After extracellular ATP binding to ATP binding site which is located at the interface of each pair of adjacent monomers, the three subunits of P2X7 trimer change the reciprocal orientation (but does not change their conformation significantly) and lead to a conformational rearrangement of the trimer. The ATP-mediated activation of P2X7 triggers ion channel pore opening(gating), which allows rapid K^+ efflux and Na^+, Ca^{2+}influx (Rassendren et al., 1997). Then the channel goes into slow desensitization phase and is followed by recovery (Coddou et al., 2011). However prolonged stimulation by ATP can induce P2X7-dependent membrane permeabilization. The secondary pore pathway permits the transmembrane fluxes of large organic molecules such as N-methyl-D-glucamine$^+$, ethidium$^+$, YO-PRO-12$^+$, lucifer yellow and carboxyfluorescein (Schilling et al., 1999). This secondary permeability pathway was thought to be unique in P2X7, but it is indicated currently that other P2X

receptors including P2X2, P2X4 and P2X5 can also permeabilize cells (Chaumont and Khakh, 2008; Compan et al., 2012). The permeabilizing process is observed consistently in P2X7 but mechanisms are not clearly understood. Some researches indicate that the long intracellular C-terminal plays a crucial role in the formation of pore (Rassendren et al., 1997; Smart et al., 2003).

P2X7 plays a pivotal role in inflammation mainly because of its unique ability to activate inflammasome. NLRP3 is a cytosolic multiprotein platform belong to NLR family and involved in many immune responses. A "two signal" model is usually used to explain NLRP3 inflammasome activation. The priming signal is provided by pathogen-associated molecular patterns (PAMPs) which promote the transcriptional induction of Toll-like receptors (TLRs). TLRs upregulate transcription of the genes encoding IL-1b and inflammasome components including NLRP3 through NF-γB pathway. Several molecular and cellular events have been proposed as second signal responsible for NLRP3 inflammasome activation independently, including K^+ efflux, Ca^{2+} signaling, reactive oxygen species (ROS), and cathepsin released from lysosome. In response to these signals, scaffold components, including the cytoplasmic receptor NLRP3, the adaptor protein ASC and the effector protein caspase-1, oligomerization and assembly. Activated NLRP3 inflammasome can induce the cleavage of pro-IL-1b and the release of mature IL-1b. P2X7 is a major trigger in this NLRP3 inflammasome activation process by forming the channel pore which allows for K^+ efflux (Gombault et al., 2012; He et al., 2016). P2X7 is also associated with a variety of cell-specific signaling pathways which are involved in inflammation, such as regulating the inflammatory cytokine production and release, including IL-1b, IL-1 receptor antagonist (IL-1Ra), IL-2, IL-4, IL-6, IL-13, interferon-inducing factor (IL-18), tumor necrosis factor-alpha (TNF-a), nitric oxide (NO), and superoxide anions.

3. AIMS OF THIS STUDY

The overall aim of this thesis was to study the biological role of P2X7 receptor in adipose tissue function.

Specifically the aims were

1) To determine the expression of AN receptors and metabolizing enzymes of macrophages, adipocytes, and endothelial cells in WAT and BAT.

2) To investigate the functional relevance of extracellular AN metabolism for obesity-associated inflammation in WAT and BAT.

3) To explore the role of extracellular AN metabolism for lipid replenishment and adaptive thermogenesis in BAT.

4) To study the effect of P2X7 ablation in general energy metabolism of lean and obese mice.

4. MATERIALS AND METHODS

4.1 Experimental mice and diets

The Animal Welfare Officers of University Medical Center Hamburg-Eppendorf approved all experimental procedures. Mice were bred and housed in the animal facility of UKE. We used age-matched (4 to 6 weeks old) male and female C57BL/6J WT mice and P2X7 KO mice which were obtained from Institute for Immunology of UKE. Mice were maintained on a standard chow diet (19.10 % protein, 4 % fat, 6 % fiber, from Altromin Spezial futter GmbH&Co, Germany) under a regular 12 hours light/12 hours dark cycle at 22 °C temperature. Control (22 °C) and cold exposure (6 °C) was performed in single cages for 24 h. High-fat diet experiments in male P2X7 KO mice were performed by feeding high-fat diet (20 % protein, 35.6 % fat, 0.3 % fiber, 23.2 % sugar, from ssniff Spezial diaeten GmbH, Germany) to 6-week old mice for 12–17 weeks in a humidity-controlled climate chamber at thermoneutral temperature (30 °C) for adipose whitening studies or at 22 °C. Body weight was measured weekly. At the end of experiments, mice were sacrificed by cervical dislocation after euthanized with CO2, and harvested tissues were either formalin-fixed for histology analyses or snap frozen in liquid nitrogen for quantitative PCR (Q-PCR) and Western blot analyses. Frozen tissues were stored at -80 °C.

4.2 Energy expenditure measurement

Metabolic rate was measured by indirect calorimetry in metabolic cages (TSE system GmbH, Germany) established in UKE animal facility. The system was operated according to the manufactures guidelines. All mice were acclimatized to monitoring cages for 48 hours prior to the beginning of physiological parameters recording. Oxygen sensors were calibrated before every new measurement. O_2 and CO_2 levels in each cage were measured for 2.5 min in each 15 min measurement interval. The levels were compared to a reference cage for calculation of O_2 consumption and CO_2 production. Food and drink intake were

measured by weighing sensors and locomotor activity was tracked with infrared light beams along X and Y axis of the cage. Mice were housed singly and maintained under a 12 - 12 hours light/ dark cycle. For gradual cold exposure studies, P2X7 KO and WT mice were acclimated at 22 °C and exposed gradually to 30 °C and the temperature was subsequently decreased by 4-5 °C (from 30 °C to 6 °C) at 7 am each day. The respiratory exchange ratio (RER) is the ratio between the amount of carbon dioxide produced in metabolism and oxygen used.

4.3 Isolation of adipocytes, macrophages, and endothelial cells from adipose tissue

WAT and BAT harvested from 6 mice were chopped thoroughly with surgical scissors and re-suspended in digestion solution. After low speed centrifugation large adipocytes were obtained in supernatant. Next, magnetic separation was performed strictly according to the manufacturer's instructions using a Magnetic Activated Cell Sorting (MACS) pro Separator (Miltenyi Biotec GmbH, Germany). The cell pellet was re-suspended in 900 µl MACS sorting buffer and incubated with 100 µl CD11b MicroBeads (Miltenyi Biotec GmbH, Germany) at 4 °C for 15 min. After centrifugation the cell pellet was re-suspended and cell suspension was applied onto LS columns (Miltenyi Biotec GmbH, Germany). The magnetically labeled CD11b+ cell fraction was collected as macrophages from LS columns. The flow through fraction was incubated with CD31 MicroBeads (Miltenyi Biotec GmbH, Germany) and applied onto LS columns to collect CD31+ endothelial cells. The last flow through fraction was obtained as adipocytes.

4.4 RNA extraction, q-PCR and RT-PCR

Organs and tissues were homogenized in TriFast (Peqlab) using the TissueLyser (Qiangen) twice at 20 Hz for 3 min. After mixing with 20 % chloroform and centrifugation for 15 min at 18,000 g, the RNA was extracted using the Nucleo Spin RNA® according to the manufacturer's protocol. RNA was quantified using NanoDrop (Thermo Scientific, Wilmington, DE) and converted to cDNA using SuperScript III Reverse Transcriptase (Invitrogen). Quantitative real-time qPCR was performed on a 7900HT Sequence

Detection System (Applied Biosystems, USA) using TaqMan Assay-on-Demand primer sets (Applied Biosystems). Cycling parameters were: 1 cycle of 95 °C for 10 m, 40 cycles of 95 °C for 15s then 60 °C for 60 s, followed by melt curve analysis. Cycle thresholds (Ct values) were normalized to those of the Tbp housekeeping gene.

Table1. TaqMan Assays:

Gene symbol	Assay ID	Gene symbol	Assay ID
Tbp	Mm00446973_m	P2rX7	Mm01199500_m1
GPIhbp1	Mm01205849_g1	P2rX5	Mm00473677_m1
Emr1	Mm00802530_m1	UCP-1	Mm00494069_m1
Adipoq	Mm00456425_m1	IL-1b	Mm00434228_m1
CD39	Mm00515447_m1	IL-6	Mm00446190_m1
CD73	Mm00501910_m1	TNF	Mm00443258_m1
P2rX4	Mm00501787_m1	NLRP3	Mm00840904_m1

4.5 Protein isolation and Western blotting

Total lysates were prepared by homogenizing various tissues in RIPA buffer (20 nM Tris-HCl pH 7.4, 5 mM EDTA, 50 mM NaCl, 10 mM Na-Pyrophosphate, 50 mM NaF, 1 % v/v Nonident, 1 mM Na_3VO_4, 0.1 % SDS, 1x Phosphatase Inhibitor Cocktail A and B) supplemented with protease inhibitors (Roche). Homogenized tissues were centrifuged at 4 °C for 10 min at 10,000 g. Protein concentrations were determined using Pierce^{TM}BCA Protein Assay Kit (Thermo Scientific) according to the manufacture's protocol.

Protein samples (30 µg per lane) were separated by SDS-PAGE in 10 % or 12.5 % polyacrylamide gels (Stacking gel: 40 % Acrylamide 6.25 mL, 1.5 M Tris pH 8.8 6.25 mL, 10 % SDS 250 µL, 10 % APS 125 µL, TEMED 30 µL, ddH2O 12 mL. Separating gel: 40 % Acrylamide 1.3 mL, 1.5 M Tris pH 6.8 1.3 mL, 10 % SDS 100 µL, 10 % APS 70 µL, TEMED 20 µL, ddH2O 7.3 mL. Running buffer: Tris-base 3.03 g, glycine 14.4 g,

SDS 1 g, ddH2O 1 L.). Proteins were transferred to a 0.45 µm nitrocellulose blotting membrane (GE Healthcare Life sciences) in blotting buffer (56.2 g glycine, 12.1 g Tris, 1 L methanol, 4 L ddH2O) using a wet electrophoretic transfer cell at 400 mA for 5 hours or at 200 mA overnight. After blotting the membrane was stained with 0.2 % Ponceau S solution (Serva) to verify protein loading. Then blots were blocked for 2h in 5 % v/v skim milk powder in TBS-T (TBS 100 mL, Tween 1 mL, ddH2O 900 mL) or PanReac Blocking buffer (AppliChem) for 2 h at room temperature, incubated for overnight with appropriate primary antibody at 4 °C and 2h with HRP-conjugated secondary antibody at room temperature. Antibodies specific for Cd39 rabbit polyclonal antibody was kindly provided by Dr. Friedrich Nolte, Department of Immunology, UKE, P2X7rabbit polyclonal antibody was kind gift of Fa Alomone Lab, UKE, P2X4 rabbit polyclonal antibody was a kind gift of Fa. Cal Biochem, UKE. P2X5 (rabbit polyclonal antibody was purchased from ThermoFisher (Cat.no.PA5-41079), CD73 rabbit polyclonal antibody from Abcam (Cat. no.Ab175396,), and the loading control, γ-Tubulin rabbit monoclonal antibody was purchased from Abcam (Cat.no.Ab179503). The secondary antibody, goat-anti-rabbit IgG horseradish peroxidase (HRP) was purchased from Bio-Rad. After washing 3 times for 10 min in TBS-T, detection was performed on Amersham Imager600 using luminal and para-hydroxycoumarinicacid–based chemiluminescence substrate.

4.6 Isolation of primary brown adipocytes

iBAT were harvested from 6-week-old mice. Tissues were then minced with scissors and digested in isolation buffer(123 mM NaCl, 5 mM KCl, 1.3 mM CaCl$_2$, 5 mM Glucose and 100 mM HEPES, PH 7.4; 2 ml/iBAT) with freshly added collagenase II (600 U/mL, Merck) and 1.5% w/v BSA for 40 minutes in a water bath (100 rpm, 37 °C). Next, the suspension was filtered through a 100 µm nylon filter and incubated on ice for 30 minutes. The upper layer (mature adipocytes) and lower layer (tissue debris) were discarded while the middle layer, which contained the stromal vascular fraction, was filtered through a 40 um nylon filter and centrifuged for 10 min at 800 g. After discarding the supernatant, the

cell pellet was resuspended in culture media (DMEM Glutamax-I 4.5 g/L glucose, 10 % FCS (sigma, #N4637 LotNr.15D230), 1 % Pen/Strep, 1 % Anti-Anti, 2.4 nM insulin (sigma, #I-9278 EW 5807) seeded in 12 well cell culture plates (10 animals per 12 well plate) and incubated at 37 °C with 5 % CO_2. Medium was changed daily and brown adipocytes were fully differentiated after 8 days.

4.7 Isolation of macrophages

Mice were euthanized by rapid cervical dislocation. The hind legs were cut off at the hip joint with scissors and the intact femurs was placed in plastic dish containing sterile PBS. Excess muscle was removed from legs by holding end of bone with forceps and using scissors to push muscle downward away from forceps.10-mL syringe was Attached to 25-G needle and filled with cold sterile wash medium (Dulbecco's phosphate-buffered saline without calcium and magnesium). Next, the needle was inserted into bone marrow cavity of femur and bone cavity was flushed with 2 to 5 mL of the wash medium until bone cavity appeared white. Wash medium was collect in a sterile 50-mL conical centrifuge tube on ice. After centrifugation at 500 g, room temperature for 10 min, supernatant was discarded and cell pellet was resuspended in macrophage complete medium. Total bone marrow progenitor cells were counted and adjusted to a concentration of ~4×10^6 /mL in macrophage complete medium. Then a total of 4×10^5 cells per sterile plastic petri dish was added in 10 ml macrophage complete medium and incubated in 37 °C, 5 % CO2 incubator.

On day 3, another 5 mL of macrophage complete medium was added to each dish. On day 7, culture supernatants was discarded and remaining adherent cells were washed with 5 mL prewarmed DPBS without calcium or magnesium. Then 3 mL Cellstrippernonenzymatic cell dissociation solution was added to each dish. After incubation for 5 min at 37 °C, cells were dislodged into a 50-mL conical centrifuge tube and an equal volume of cold DMEM/F12-10 medium was added. Cells were resuspended in 3 to 5 mL DMEM/F12-10 medium after centrifugation for 10 min at 400 g, 4 °C. At this time the cells were essentially 100 % macrophages, with the yield being $7.5–15 \times 10^7$

macrophages per mouse.

4.8 Isolation of T cells

Kidney, interscapular and gonadal fat pads from high-fat-diet mice were harvested and the tissue was gently disrupted in PBS containing 5 % heat-inactivated fetal bovine serum (HIFBS) on ice. Kidney cells and adipocytes were passed through a 40µm nylon cell strainer (BD Biosciences) and collected in PBS. $CD4^+$ and $CD8^+$T-cells were isolated with mouse CD4 and CD8 subset column kit following the manufacturer's protocol. The purity of $CD4^+$ and $CD8^+$T-cells after isolation was 95 % as measured by flow cytometry using anti-CD4 and anti-CD8 antibody, respectively. Cells were washed and resuspended in RPMI 1640 containing 10 %HIFBS and 1 % antibiotic-antimycotic solution.

4.9 Fluorescence-activated cell sorting

T-cells (0.5×10^6) in 100 µM PBS with 1% HIFBS (fluorescence-activated cell sorting [FACS] buffer) were labeled with 0.25 µg each of FITC-labeled anti-mouse CD69 and PE-labeled anti-mouse CD4 and CD8 antibodies or FITC- and PE-conjugated isotype control antibodies at 4°C for 30min. Stained cells were washed with 10-fold excess volume of FACS buffer and resuspended in PBS containing 1 % paraformaldehyde. The fluorescence intensity was measured by collecting a minimum of 10,000 events using a BD Biosciences FACS-Calibur dual laser benchtop flow cytometer using Cell Quest software (Becton Dickinson) and analyzed using FlowJo software (Treestar,San Carlos, CA).

4.10 Blood tests and analytical measurements

Plasma glucose, cholesterol and triglyceride levels were measured using the Glucose (GO) Assay Kit (Sigma), the Cholesterol CHOD-PAP kit (Roche), the Triglyceride GOP-PAP kit (Roche), respectively. They were adapted to 96-well microtiter plate according to manufacturer's instructions. Ultra Sensitive Rat Insulin ELISA kit (Crystal Chem) was

used for the quantitative determination of insulin in mouse plasma.

To determine glucose tolerance, mice were fasted for 16h followed by an intraperitoneal injection of glucose (Sigma) at 1 g/kg body weight. Blood samples were collected at 0, 15, 30, 60, 90, and 120 min from tail. Glucose levels were measured using Accu-chek Aviva (Roche). Supernatant glycerol and free fatty acids (FFA) levels were determined using Glycerol Assay Kit (Sigma) and NEFA-HR (2) (Fujifilm), respectively.

4.11 Tissue Histology

Adipose tissues were fixed in 3.7 % formaldehyde for 24h, embedded in paraffin, and sectioned by the Leica RM 2245.The samples were hydrated as follows: the slides were transferred through three changes of 100 % ethanol for 2 min per change. Thereafter, transferred to 95 % ethanol for 2 min and to 70 % ethanol for 2 min, the samples were stained in hematoxylin solution for 3 min and in working eosin Y solution for 2 min. Next, the samples were dehydrated by ethanol as follows: transferred through 95 % ethanol for about 2 min and two changes of 100 % ethanol for 2 min per change. Then, the samples were cleared in three changes of xylene for 2 min per change. A drop of Permount was placed over the tissue on each slide and a coverslip was placed. High resolution digital images were taken using the Nikon eclipse Ti Microscope.

4.12 Statistical analysis

Results are expressed as mean±SEM. Comparisons between groups were made using either unpaired, two-tailed Student t test of the SPSS software for two-group comparisons or the two-way ANOVA test with the Bonferroni post-tests of the PRISM software for multi group comparisons. P＜0.05 was considered statistically significant.

5. RESULTS

5.1. Expression of purinergic receptors and metabolizing enzymes of adipose tissue

Thermoregulation is the capacity of an organism to maintain its relatively constant core body temperature. The metabolic rates of these organisms are related to ambient temperature. In this regard, thermoneutral zone is a state of thermal balance between an organism and its environment when extra energy needed to defend body temperature is minimal. In mice, the lower critical temperature of thermoneutral zone is 30 °C (Cannon and Nedergaard, 2004). At this temperature mice demonstrate their basal metabolic rate. At ambient temperatures outside the thermoneutral zone, a large fraction of total energy is used for thermoregulation. To note, laboratory mice are almost always housed at mildly cold temperatures (22-24 °C). Upon mild cold exposure mice initially defend their body temperature through many mechanisms such as vasoconstriction, piloerection, lower sweat rate, and conscious and unconscious behavioral adaptations. If these adjustments are insufficient to maintain temperature, involuntary shivering is triggered to increase endogenous heat production. However, after a prolonged time in cold, mice demonstrate a high metabolic rate through non-shivering thermogenesis. The classical cold-induced non-shivering thermogenesis is entirely brown adipose tissue dependent.

In order to determine the expression of purinergic receptors (P2rX7, P2rX4, P2rX5) and metabolizing enzymes (CD39, CD73) in WAT and BAT under different environment temperature conditions, I housed C57BL/6J WT mice at room temperature (22 °C), or thermoneutrality (30 °C) for 1 week . To stimulate browning in BAT and WAT, mice were housed for 1 day or 1 week at 6 °C. After that mice were sacrificed by cervical dislocation, inguinal WAT (iWAT), gonadal WAT (gWAT) and interscapular BAT (iBAT) was harvested. Expression of indicated genes was relative to mock-controls (22 °C for 1 week) (Fig 3). CD39 mRNA level was upregulated significantly in iBAT after 1 week
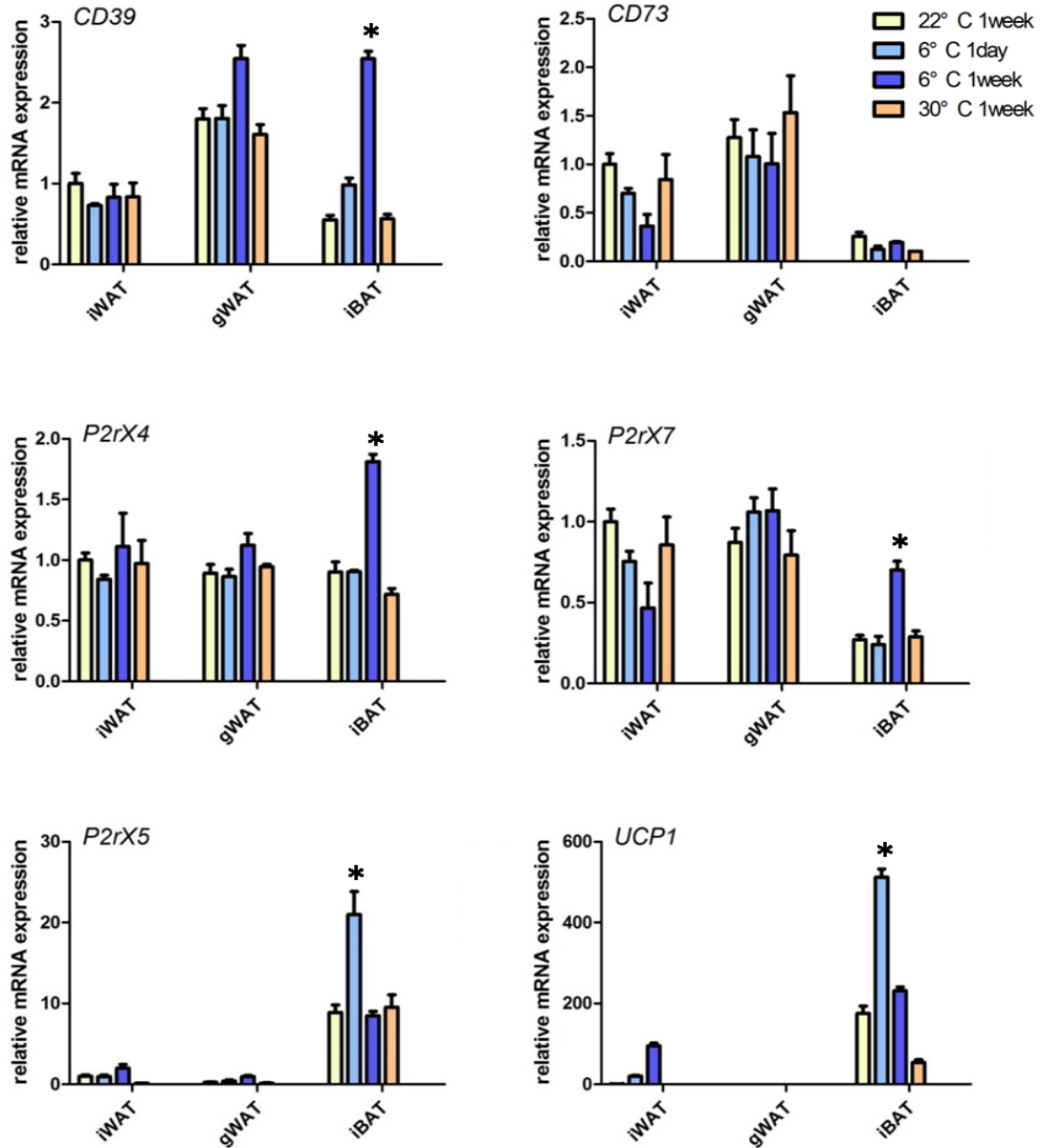
Figure 3. **mRNA expression levels of CD39, CD73, P2rX4, P2rx5, P2rx7 and UCP1 in iWAT, gWAT and iBAT**. *Male WT mice were housed at 22°C, 6°C, or 30°C for 1 week or at 6°C for 1 day. n=4 mice per group. Expression of indicated genes relative to controls (22°C for 1 week) was determined using specific TaqMan® probes for the indicated genes. CD39 expression of iBAT increased after 1 week cold. CD73 did not change significantly while P2rX4 and P2rX7 had higher expressions in iBAT after short cold stimulation. P2rX5 had remarkably higher expression in BAT than WAT and increased significantly after 1 day cold exposure. Data are presented with mean±SEM. *P< 0.05.*

cold exposure. CD73 expression in gWAT showed a trend towards decreased expression after short and long time cold stimulation. Both P2rX4 and P2rX7 mRNA expression increased after 1 week cold exposure in BAT. These cold induced alterations suggest a role of these receptors and enzymes in activating BAT. Interestingly, P2rX5 was remarkably more highly expressed in BAT than WAT and short cold exposure lead to an increase in P2rX5 expression in BAT. P2rX5 displayed a gene expression pattern similar to UCP1, which is a marker gene for brown adipocyte, indicating P2rX5 may participate in browning of adipose tissue or has cooperation with UCP1 in BAT function. However, in this experiment 7-day cold exposure did not affect gene expressions of both P2rX5 and UCP1. After housing at thermoneutrality (30 °C) for 1 week, WT mice had no alternations in mRNA expression of CD39, CD73, P2rX4, P2rx5, and UCP1.

5.2. FACS analysis of tissues from obese WT and P2X7 KO mice

To note, P2X7 KO mice used in my experiments were generated from C57BL/6J strain background. C57BL/6J mouse has a natural mutation at position 451 in the cytoplasmic tail of P2X7 coding region. The distribution of this mutated 451LSNP allele differs in different mouse strains. BALB/c mice were demonstrated to carry 451P SNP in P2rX7 whereby T cells have higher sensitivity to eATP than C57BL/6J mice (Adriouch et al., 2002). Transfection studies in HEK-293 cells indicated 451L allele impaired markedly ATP induced P2X7 channel and pore function. Another study found P451L polymorphism in the mouse P2X7 receptor appears to inhibit downstream signaling independently of ion channel activation, such as reduced dye uptake and calcium flux (Young et al., 2006). It has already been pointed out that the attenuated phenotype of the P451L polymorphism may underestimate the P2X7 receptor-deficient phenotype in the B6 wild-type mouse.

There are currently two strains of P2X7 KO mice available, which were generated by GlaxoSmithKline (GSK) and Pfizer. The GSK mice line was generated by inserting a lacZ transgene and neomycin cassette into exon 1 of P2rX7, whereas the Pfizer KO was

generated by inserting a neomycin cassette into exon 13, replacing part of the C terminus of the receptor. Both strains have been indicated to escape deletion. In GSK mice, T cells displayed even higher levels of P2X7 activity than that of control mice (Taylor et al., 2009). It is suggested that because these cells are always compared with wild-type C57BL/6 animals, which have P2X7 function dependent on normal levels of the low-activity 451L allele. Pfizer KO mice are not null for P2X7 receptor expression but express ΔC variants with reduced function (Masin et al., 2012). Nevertheless these two models have been extensively used for demonstrating P2X7 functions especially in inflammation. The mice I used were Pfizer KO mice with the vector disrupting exon 13 of the P2rX7 gene. The P2rX7 TaqMan probe used for quantitative PCR to detect P2rX7 mRNA expression was attached to exon 1, and because of a number of variants in P2rX7, P2rX7 mRNA still could be detected in some tissues and cells. However, FACS was used to verify the ablation or decrease of P2X7 protein in P2X7 KO mice (Figure 4).

After harvesting organs from obese WT and P2X7 KO mice, I isolated T cells from kidney, iBAT, and gWAT and separated CD4$^+$ and CD8$^+$ T cells. For FACS described here I used T cell surface marker CD69, which is an early marker for T cell activation, along with P2X7 antibody for determination. As shown in the image, CD69 is on the X-axis and P2X7 is on the Y-axis. The flow cytometry plots in the upper two zones represent P2X7 positive cells. The results show deficient expression of P2X7 protein in T cells from KO mice. Thus, we could confirm the ablation of P2X7 protein in P2X7 KO mice.

5.3. Expression of purinergic receptors and metabolizing enzymes of macrophages, adipocytes and endothelial cells in adipose tissue

ATP is generally released by sympathetic nervous system as well as other cells including adipocytes, endothelial cells, and immune cells under physiological and pathophysiological conditions, and participates in modifying a wide range of cell functions, that builds up the purinergic signaling network in adipose tissue. However, the mechanism of how this network works currently remains to be explored. Few studies investigated the expression of AN receptors and enzymes in different cell types of adipose
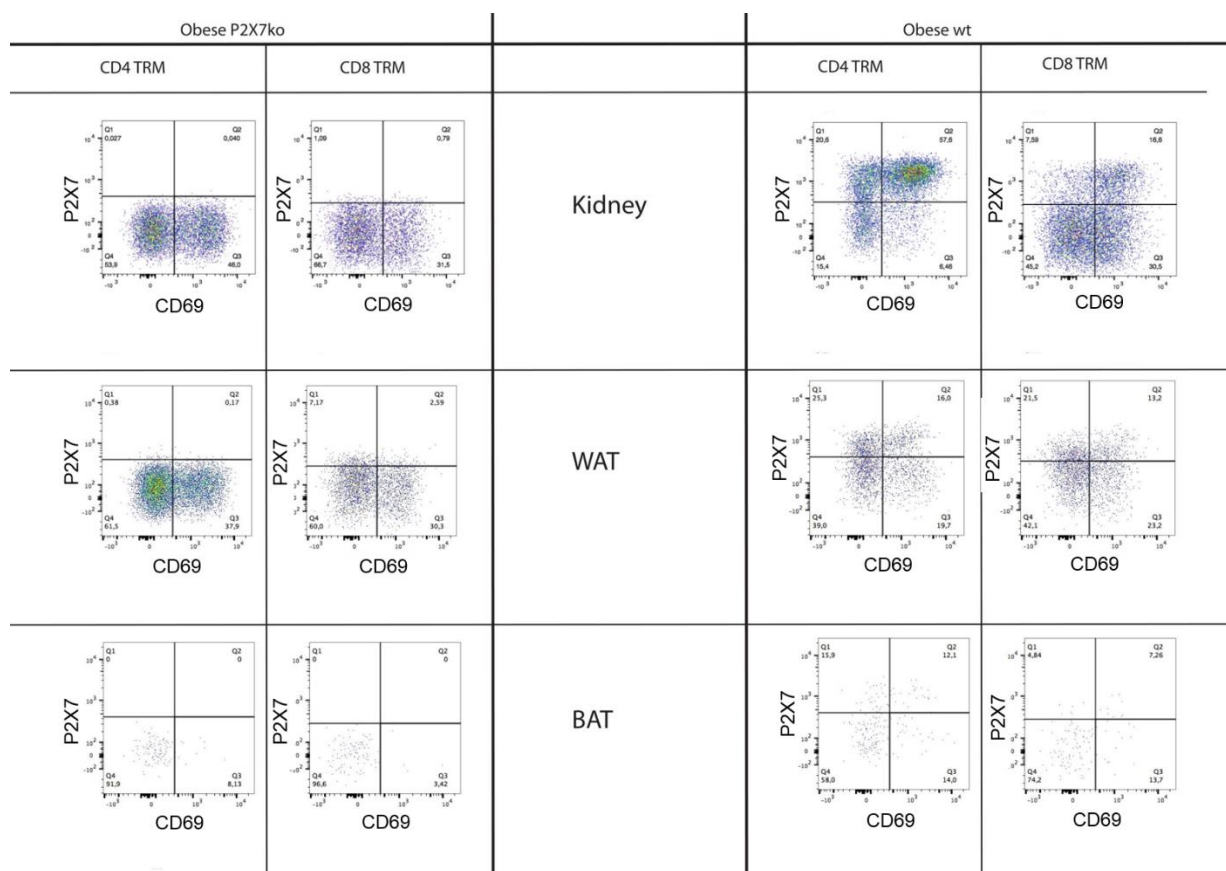
Figure 4. FACS analysis of kidney, iBAT and gWAT from P2X7 KO mice fed on HFD for 16 weeks. *T cells were initially gated on a CD4⁺ or CD8⁺ population and then the proportion of CD69+P2X7+ were determined. P2X7 protein were abolished in T cells from P2X7 KO mice.*

tissue. To determine the relative expression of AN receptors and enzymes in adipose tissue, I separated different cell types from iBAT and subcutaneous WAT (subWAT) of wild-type mice and P2X7 KO mice housed at room temperature or after 1-day cold exposure via MACS technique.

MACS is an antibody-based cell separation process to enrich a specific cell population directly out of whole tissue. The antibodies conjugated to magnetic nano-sized beads recognize antigens (receptors) expressed on the cell surface. The magnetic particle-cell

complex passes through the column which is placed between permanent magnets so that the tagged cells can be captured by the column. In my experiments large adipocytes, adipocytes, endothelial cells and tissue-resident macrophages were isolated cells from adipose tissue using a procedure presented in Fig.5. First, after collagenase digestion of subWAT and iBAT (harvested from 6 mice), large adipocytes were separated by low speed centrifugation. Next, CD11b$^+$ macrophages were magnetically labeled with a cocktail of biotin-conjugated antibodies against CD11 band Anti-Biotin MicroBeads. The cell suspension was applied onto a MACS Column and the labeled cells were collected after removing the column from the magnet. Then the unlabeled flow-through fraction was incubated with CD31 MicroBeads for subsequent positive selection of CD31$^+$ endothelial cells. The last flow through fraction was obtained as adipocytes.
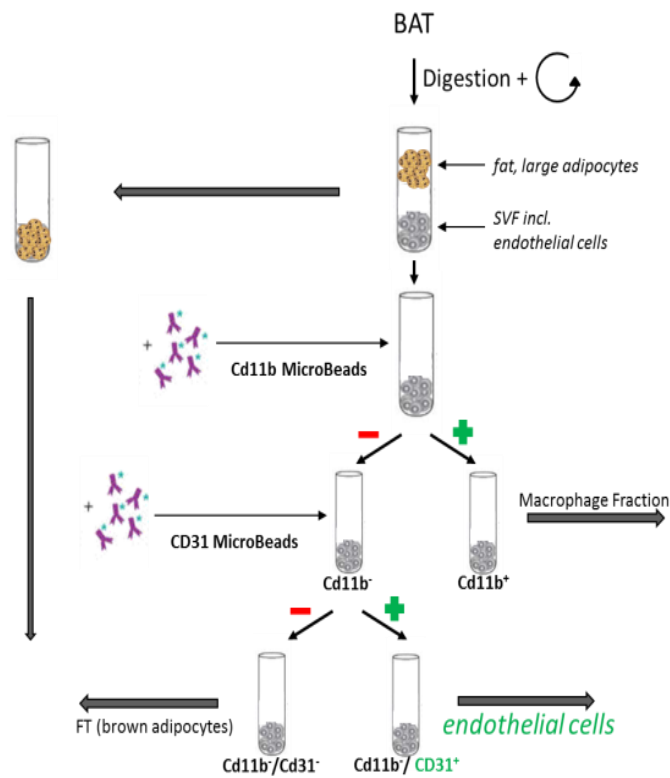

Figure 5. Cell separation procedures of large adipocytes, adipocytes, endothelial cells and tissue-resident macrophages from adipose tissue utilizing MACS. *MACS system is based on the cell surface markers of different cell types in adipose tissue: macrophages express CD31 and CD11b, and endothelial cells express only CD11b while adipocytes are both CD11b and CD31*

negative. During incubation with a cell suspension, the antibody/bead complex binds to cells expressing the corresponding epitope. When the cell suspension was placed into a magnetic field, cells labeled by magnetic MicroBeads could bind to LS columns while unlabeled cells were collected as flow through. The sample was subsequently removed from the magnet and eluted by MACs buffer to collect the positively labeled cells.

P2X7 KO and WT mice were housed at either cold (6 °C) or room temperature (22 °C) for one day. I harvested iBAT and subcutaneous WAT from each group. By using MACS technique we succeeded to isolate relatively pure fraction of different cell types based on the expression of specific markers for adipocytes (Adipoq), endothelial cells (Gpihbp1) and tissue-resident macrophages (Emr1) (Fig.6A-C).

CD39 was primarily expressed by macrophages and endothelial cells (Fig.6D). One-day cold stimulation increased the expression of CD39 in endothelial cells from subWAT and macrophages from iBAT. CD73 mRNA was detected in all cell types investigated (Fig.6E). The expression of CD73 was significantly increased in endothelial cells and macrophages from subWAT after cold exposure. P2rX7 expression was enriched in macrophages (Fig.6F). As explained before, because of the technical reason I still observed P2x7 expression in P2X7 KO cells. However, P2rX7^{-/-} macrophages appear to have a decreased P2rX7 mRNA level. P2rx4 was expressed in macrophages and adipocytes and had an induction in macrophages from iBAT after cold exposure (Fig.6G). Notably, I found P2rX5 expression is remarkably higher in brown adipocytes than white adipocytes and other cell types (Fig.6H), which is also in accordance with the expression of UCP1 (Fig.6I). Both P2rX5 and UCP1 had significant upregulation in mRNA level after cold stimulation.
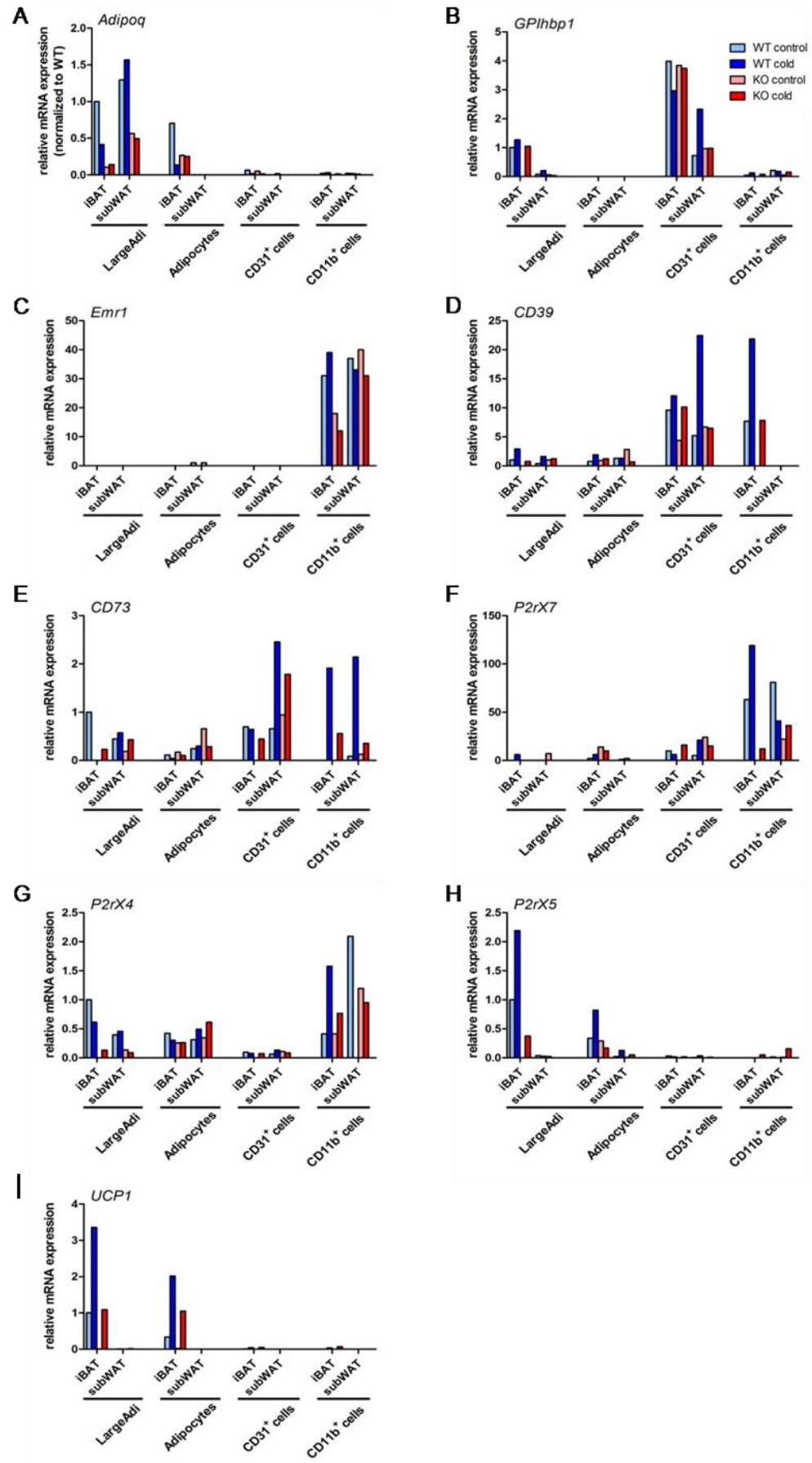
Figure 6. Gene expression of *Adipoq, GPIhbp1, Emr1, CD39, CD73, P2rX4, P2rx5* and *Ucp1* in cell fractions from adipose tissue with MACS technology. *Male WT and P2X7 KO mice were housed at 22 ℃ or 6 ℃ for 24 hours. n=6 mice per group. Expression of indicated genes relative to controls (WT mice at 22 ℃) was determined using specific TaqMan® probes for the indicated genes. Adipoq, Gpihbp1 and Emr1 were used as marker genes to confirm the isolation of adipocytes, endothelial cells and tissue-resident macrophages, respectively. The relative distribution of genes in adipose tissue is showed in figure. In subWAT CD73 had increased expression in endothelial cells. In iBAT, CD39 and P2rX4 had a tendency for increased expression in macrophages. Notably, P2rX5 showed remarkably higher expression in iBAT and was increased significantly after cold exposure. Data are presented with mean±SEM.*P< 0.05.*

5.4. Effect of P2X7 deficiency on energy expenditure in lean mouse

Next I studied whether P2X7 plays an important role in regulating whole body energy metabolism in lean mouse at thermoneutral and cold conditions. Metabolic cages were used to record respiratory O_2 consumption, CO_2 production, activities, and food and drink intake every three minutes. P2X7 KO and WT mice were housed in cages for 1 week with a gradual decrease in temperature from 30 ℃ to 6 ℃ (5-6 ℃ each day). Results showed both P2X7 KO and WT mice displayed higher energy expenditure during day and under cold condition than at night and under warm condition, respectively. However, there was no significant difference in O_2 consumption, CO_2 production, accumulation of O_2 consumption and CO_2 production, and respiratory exchange ratio (RER) between P2X7 KO mice compared to WT controls (Fig.7A-E). P2X7 KO mice had lower physical activities than WT mice, but the difference was not significant (Fig.7F). Furthermore, there was no significant difference in food and drink intake between P2X7 KO and WT control mice (Fig.7G-H)
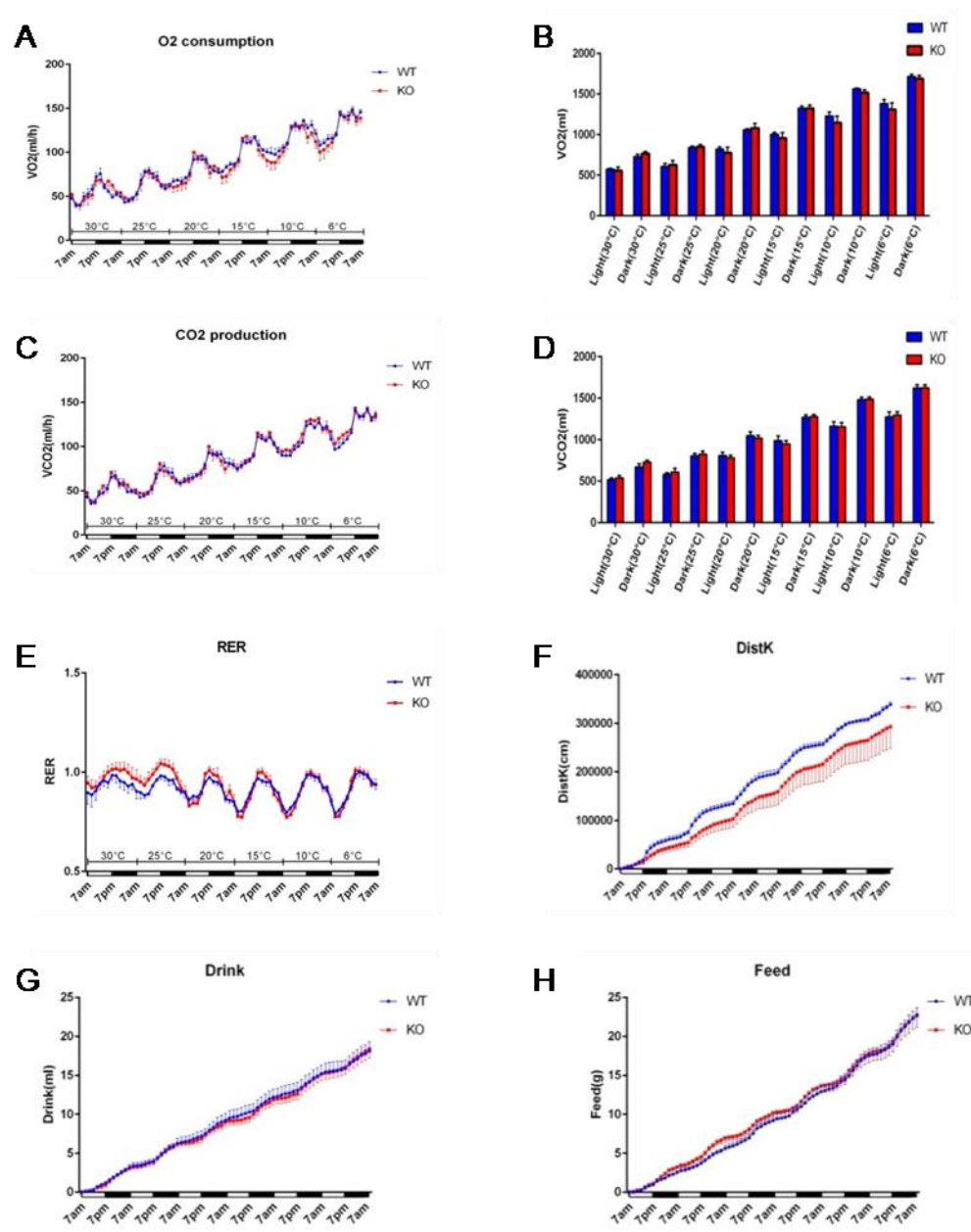
Figure 7. Systematic energy expenditure of lean WT and P2X7 KO mice. *Female WT and P2X7 KO mice were kept in metabolic chambers for one week. 12-12 hour day and night cycle and decreased temperature from 30°C to 6°C were determined by TSE system. Oxygen consumption (A), accumulation of oxygen consumption in day and night time (B), carbon dioxide production(C), accumulation of carbon dioxide production in day and night time (D) and RER (E) did not exhibited significant difference between WT and P2X7 KO mice. P2X7 KO mice had lower horizontal and vertical movement than WT mice but the difference was not statistically significant*

(F). Drink and food intake (G and H) were similar between two groups. For all experiments, n=6 mice per group. Data are presented as mean±SEM.*P< 0.05

5.5. Effect of P2X7 deficiency on energy expenditure in diet-induced obese mouse

Adipose tissue dysfunction is closely related to many metabolic disorders such as obesity, insulin resistance, and hyperglycemia. Since P2X7 is a key receptor in inflammatory response and widely expressed in immune cells, endocrine cells, and adipocytes, it has been considered to participate in the pathogenic process of many metabolic disorders like obesity and diabetes.

The diet-induced obese mice model (DIO model) is a model wherein obesity is induced by high-fat or high nutrient-density diets. It is intended to mimic the most common cause of obesity in humans and used as a tool to study obesity and related disorders such as insulin resistance. In order to determine the effect of P2X7 deficiency on diet-induced obesity, we subjected P2X7 KO and WT mice to HFD feeding regimen at room temperature (22 °C) and thermoneutrality (30 °C) for 12 weeks and 16 weeks, respectively (The HFD was terminated in mice of room temperature group due to the energy expenditure experiment in 12th week). After long period HFD feeding, P2X7 KO mice showed a trend towards decreased body weight than WT controls, especially at thermoneutral temperature (30 ℃)(Fig.8A). The steep decline in body weight at 12th week in mice at thermoneutral temperature (30 ℃) was due to the glucose tolerance test made on mice. We also calculated the body weight gain of each group. P2X7 KO mice showed a trend towards reduced body weight gain than WT controls at room temperature (22 °C) and thermoneutral temperature (30 ℃) (Fig.8B).

We next repeated the energy expenditure experiments in diet-induced obese P2X7 KO and WT mice fed HFD for 12 weeks. Although upon cold exposure, P2X7 KO mice exhibited reduced O_2 consumption than WT mice at some time intervals (Fig.9A) and decreased food intake (Fig.9G), CO_2 consumption and respiratory exchange ratio were
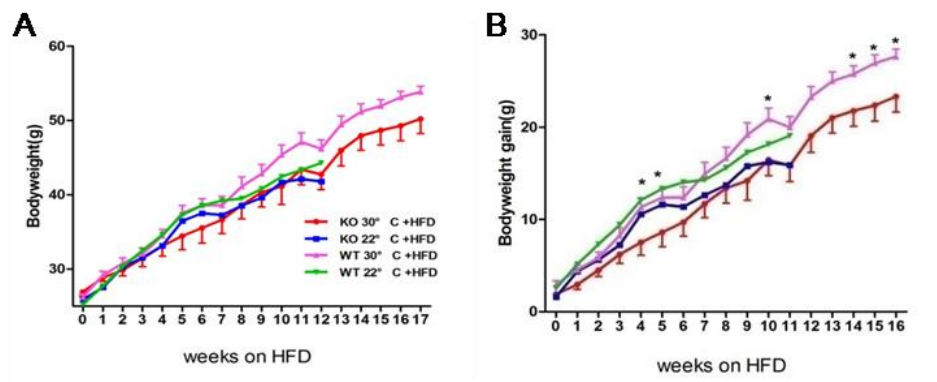
Figure 8. Body weight (A) and body weight gain (B) in male WT and P2X7 KO mice fed HFD at 30 °C or 22 °C. *P2X7 KO mice exhibited no significant difference in body weight compared to WT controls. P2X7 KO mice showed decreased body weight gain at 30 ℃. For all, n=6-9 mice per group. Data are presented with mean±SEM.*P< 0.05*

not significantly different (Fig.9C, E). Similar to lean P2X7 KO mice, no significant difference was observed in water intake and physical activity (Fig.9F, H).

Furthermore, glucose tolerance tests were performed in 12 weeks of HFD fed mice housed at thermoneutral temperature (30 ℃) using 1g glucose/kg after 16 hour fast, both P2X7 KO and WT mice exhibited hyperglycemia, but glucose tolerance test did not show significant effect on insulin sensitivity in P2X7 deficient mice (Fig.10A). Plasma parameters indicated that P2X7 deletion did not have a significant effect on plasma glucose, insulin, TG, and cholesterol levels (Fig.10B-E).
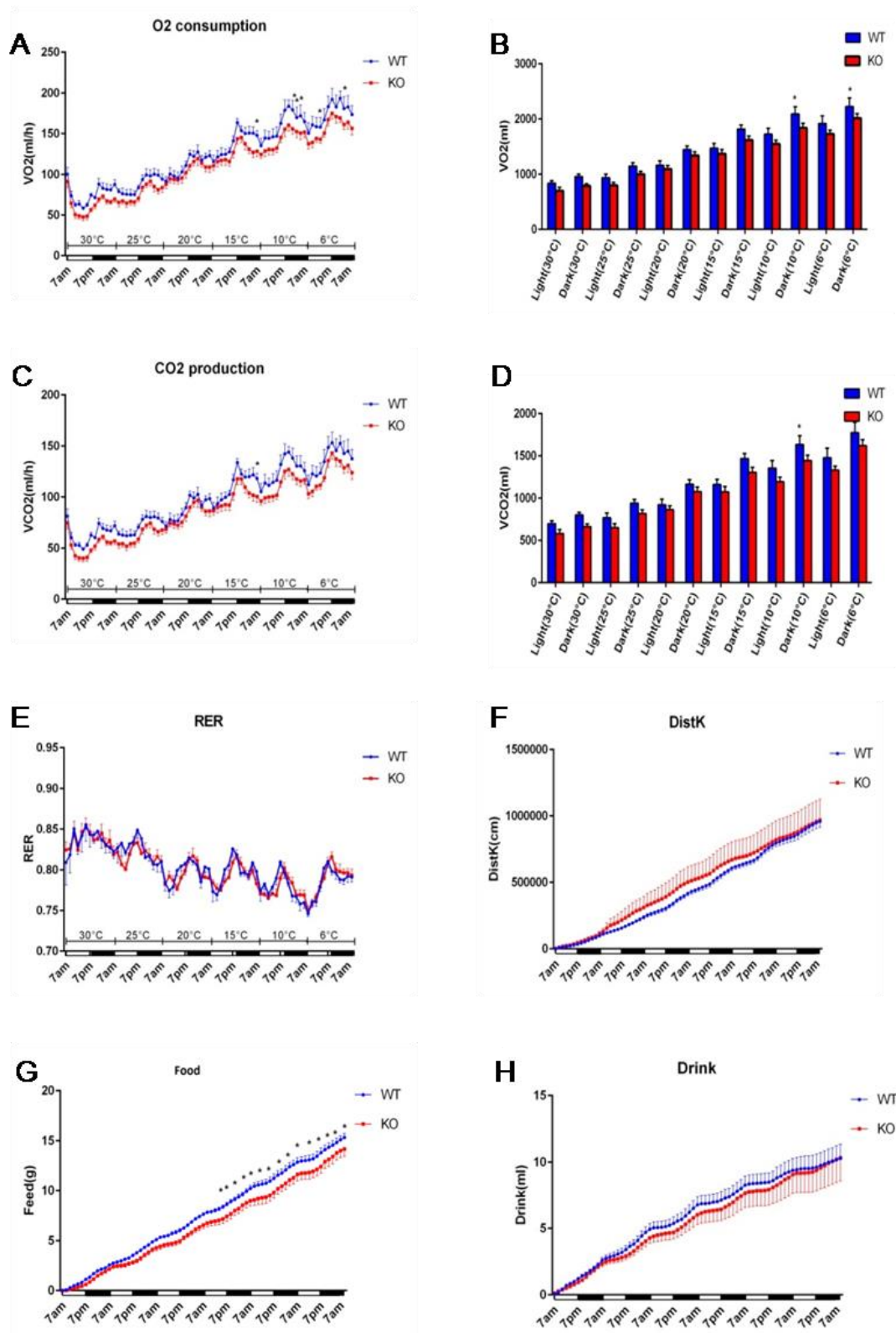
Figure 9. Systemic energy metabolism in obese P2X7 KO mice. *Energy expenditure experiment was repeated as before (see figure.7). Male WT and P2X7 KO mice were kept in*

metabolic chambers for one week with 12-12 hour day and night cycle.   Decrease in housing

temperature from 30 °C to 6 °C was determined by TSE system. P2X7 KO mice exhibited reduced

O_2 *consumption and accumulation of* O_2 *consumption than WT mice at some time intervals (A).*

CO2 production (C), accumulation of CO_2 *production in day and night time (D) and RER (E) did*

not exhibit significant difference between WT and P2X7 KO mice. P2X7 KO mice had lower food

intake than WT mice (G). Activities and drink intake (F and H) were similar between two groups.

For all, n=6 mice per group. Data are presented as mean±SEM.*P< 0.05

Figure 10.Glucose tolerance test and plasma parameters of DIO P2X7 KO mice. *Glucose tolerance test with 1g glucose/kg after 16 hour fast upon 12 weeks of HFD feeding showed no difference in insulin sensitivity between WT and P2X7 KO mice (A). P2X7 deficiency did not affect plasma glucose, insulin, TG and cholesterol levels (B-E). Data are presented with mean±SEM.*P< 0.05*

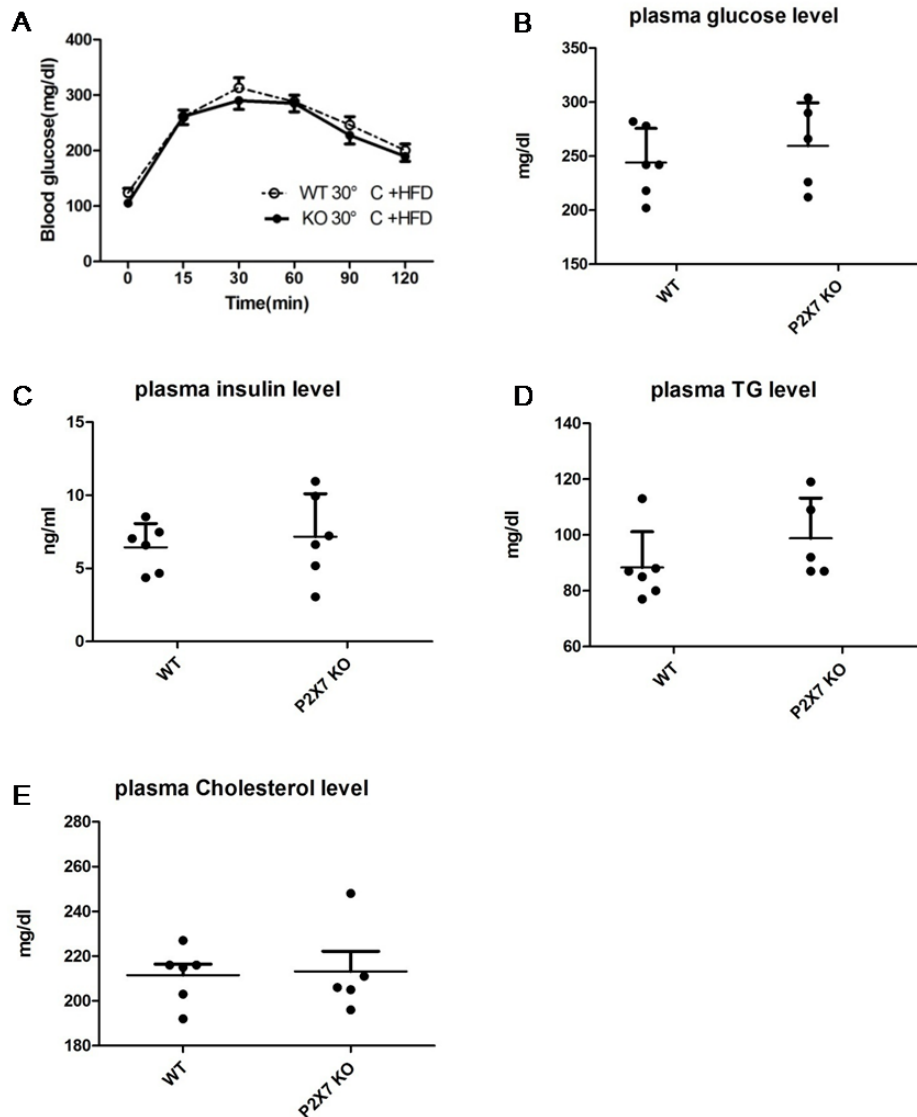## 5.6. Histology and Western blot analysis in obese WT and P2X7 KO mice

After 16 weeks of HFD feeding liver, spleen, gonadal WAT, inguinal WAT, subcutaneous BAT and supraclavicular BAT was harvested from WT and P2X7 KO mice. Hematoxylin-eosin (H&E) staining was used to analyze morphology of adipose tissue in mice and representative microphotographs are shown below. Histological results revealed no significant morphological differences in gWAT, iWAT, or scBAT (Fig.11A) in P2X7 KO mice compared to WT controls.

Western blot analysis showed reduced P2X7 protein (~ 80 KDa band) levels in various tissues tested e.g. gWAT, iWAT, iBAT, liver, and spleen of P2X7 KO mice (Fig.11B). Interestingly, relative protein levels of P2X4 and P2X5 was higher in iBAT than other tissues in WT mice. P2X7 KO mice exhibited reduced P2X4 protein levels while P2X5 protein level was increased in the absence of P2X7 receptor.

5.7. Effect of P2X7 deficiency on inflammation

Previous studies have demonstrated an important role of ATP-P2X7 axis in inflammatory responses (Sun et al., 2012a). After activated by extracellular ATP, P2X7 receptor opens its channel pore which leads to K^+ inward flux. The low intracellular K^+ concentration triggers the maturation of NLRP3 inflammasome as the second signal, thereby activates caspase-1 cleavage and mature IL-1β release. IL-1β is an inflammatory cytokine which has been associated with insulin resistance during obesity. To note, ablation of NLRP3 in
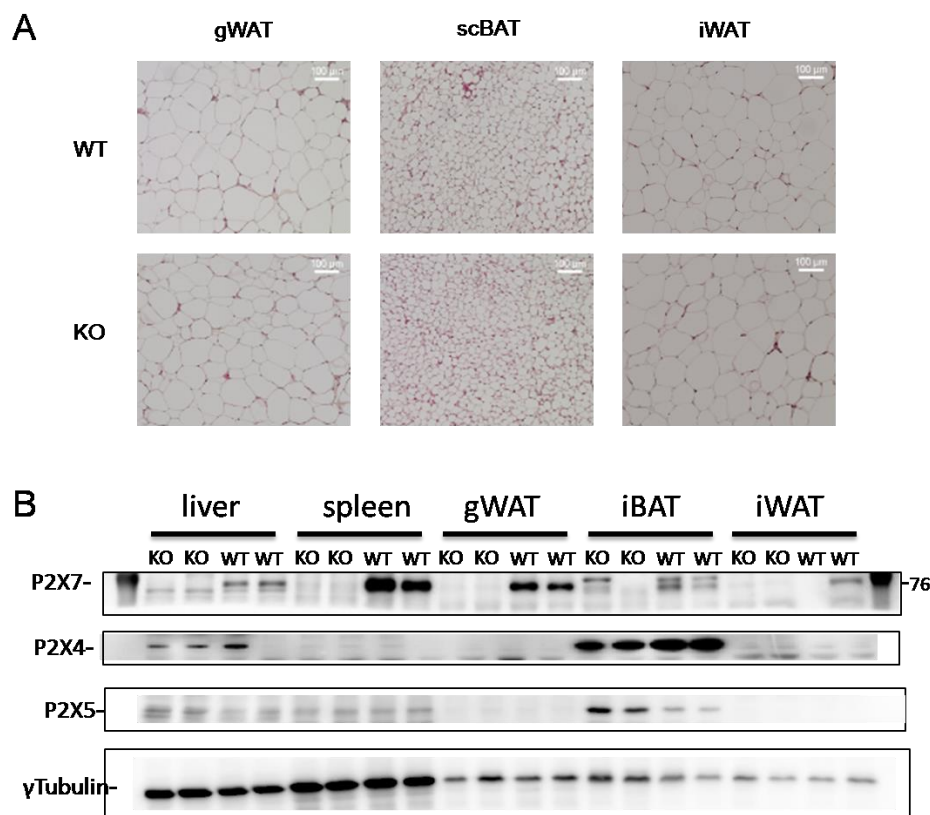
Figure 11. Histology and Western blot analysis in P2X7 KO mice fed HFD for 16 weeks.

Representative microphotographs of mouse gWAT, scBAT and iWAT after H&E staining. P2X7 KO mice exhibited no significant morphological differences compared to WT adipose tissue (A). Protein used for Western blotting was extracted from liver, spleen, gWAT, iBAT and iWAT of 16-week HFD fed WT and P2X7 KO mice (B). P2X7 KO mice displayed reduced P2X7 protein levels in various tissues. Among the various fat depots tested, P2X4 and P2X5 protein showed a higher expression in iBAT. In P2X7 KO mice, P2X4 protein showed reduced expression in iBAT while P2X5 level was increased. Tubulin was used as loading control.

mice has protective function against obesity-induced inflammation in adipose tissue and liver (Vandanmagsar et al., 2011).

Here I determined the gene expressions of purinergic receptors, ectoenzymes and inflammatory cytokines in obese mice. In gWAT, I observed significant reduction of P2rX7 level in P2X7 KO mice. In other tissues, however, there was no difference in P2rX7 mRNA expression between P2X7 deficient mice and WT controls. In gWAT, gene expression of CD39 and P2X4 was reduced in P2X7 KO mice (Fig.12).
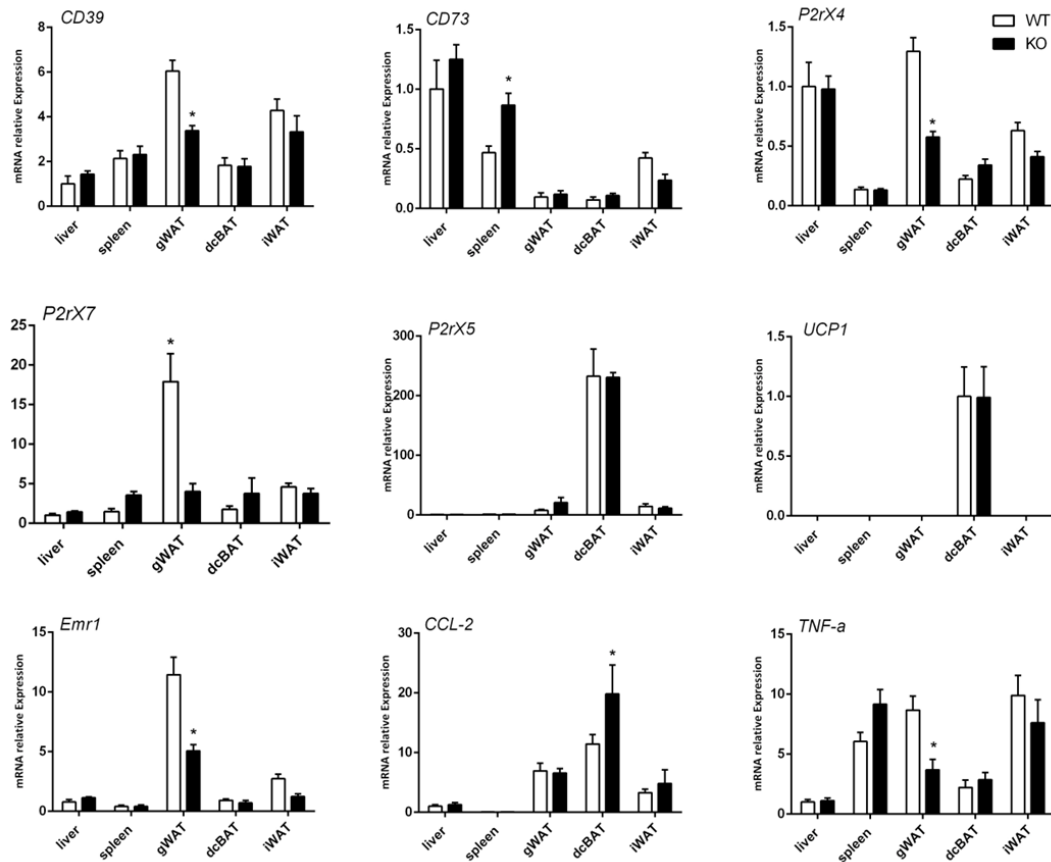
Figure 12. mRNA expression levels of CD39, CD73, P2rX7, P2rX4, P2rX5, UCP1 and inflammatory genes in liver, spleen, WAT and BAT of DIO WT and P2X7 KO mice. *n=6 mice per group. Expression of indicated genes was relative to controls. Gene expression of CD39 and P2rX4 was reduced in gWAT of P2X7 KO mice. P2rX5 level was remarkably higher in dcBAT than other tissues. Emr1 and TNF-α were reduced in gWAT while CCL-2 level increased in dcBAT of P2X7 KO mice. Data are presented with mean±SEM.*P< 0.05*

EGF-like module-containing mucin-like hormone receptor-like 1 (Emr1) is a widely used marker for murine macrophages. Tumor necrosis factor-alpha (TNF-α) is the cytokine involved in systemic inflammation which is primarily released by active macrophages. TNF-α can affect multiple adipose functions including lipogenesis, adipogenesis, thermogenesis as well as endocrine function (Cawthorn and Sethi, 2008). The chemokine (C-C motif) ligand 2 (CCL2), which is also referred to as monocyte chemoattractant protein 1 (MCP1), is known to be associated with macrophages/monocytes recruitment and regulation. CCL2 binds to its receptor CCR2 and regulates migration and infiltration of monocytes/macrophages. All of those molecules may be released by active immune cells infiltrating obese adipose tissue and lead to local and generalized inflammation. Gene expression of *Emr1* and *TNF-α* was reduced in gWAT indicating reduced adipose inflammation in P2X7 KO mice compared to WT controls upon HFD feeding.

5.8. Gene expression of purinergic receptors and enzymes in activated murine brown adipocytes and macrophages treated with CL, adenosine and ATP *in vitro*

There are three types of adrenergic receptors: α1, α2 and β in adipose tissue. Adrenaline and norepinephrine binding to these receptors regulate different signaling pathways. β-adrenergic receptors, which are members of the large family of G protein coupled receptors (GPCR), can be subdivided into β1, β2 and β3 receptors. Of the three subtypes, β3-ARs are found predominantly in adipose tissue and skeletal muscle. It has been demonstrated that β3-ARs play a vital role in adipose tissue functions. Administration of CL-316,243, which is considered as the most selective β3 agonist, leads to the stimulation of sympathetic nervous system and marked increases in thermogenesis and lipolysis in adipose tissue (Grujic et al., 1997).

Adenosine is released in adipose tissue both from breakdown of extracellular ATP and efflux from adipocytes. Some studies indicated that noradrenaline also increases adenosine in extracellular space, suggesting a network between catecholamine and

adenosine signaling. Adenosine is known to inhibit lipolysis in WAT. However, recent research found that adenosine can stimulate lipolysis in human and murine brown adipocytes via A2A receptors (Gnad et al., 2014). *In vitro* experiment showed that this adenosine-induced lipolysis is concentration dependent. When treated with increasing concentration of adenosine, increased lipolysis can be observed.

As mentioned, the "two signal" model has been used to analyze inflammasome activation. Lipopolysaccharide (LPS) is a well-known PAMP which can provide the primer signal of upregulating the transcription of genes of inflammasome components by activating toll-like receptor 4. Additionally, ATP may be quickly hydrolyzed in extracellular space. Therefore, a high ATP level was required for P2X7 activation (~5 mM).

Primary brown adipocytes were isolated from WT mice brown adipose tissue. After culture and differentiation, they were treated with CL (50nM), adenosine (1nM) or LPS+ATP (LPS: 0.1μg/ml, ATP: 100mM) for 4 h. Relative mRNA expressions are shown in Figure 13A. We could observe a significant reduction of P2rX7 level induced by LPS+ATP treatment when compared with controls (mock). Though CL induced significant increase in UCP1 gene level as expected, CL and other treatments did not alter expression of P2rX5 when compared to control (mock). During the experiment, cell supernatants were collected to determine lipolysis of brown adipocytes under different conditions (Fig. 13B). Lipolytic response to CL was observed with increased free fatty acid (FFA) and glycerol concentrations. However, adenosine did not affect lipolysis in brown adipocytes.

I also performed a time course experiment with CL. Brown adipocytes were harvested at 2, 4, and 6 h of CL treatment. Interestingly, in contrast to the increased expression of UCP1 induced by CL activation, P2rX5 mRNA level had a slight increase at 2 h, but decreased at 4 and 6 h of CL treatment (Fig.14). Though these alterations were not statistically significant, they still indicated potential influence of β3-ARs activation on
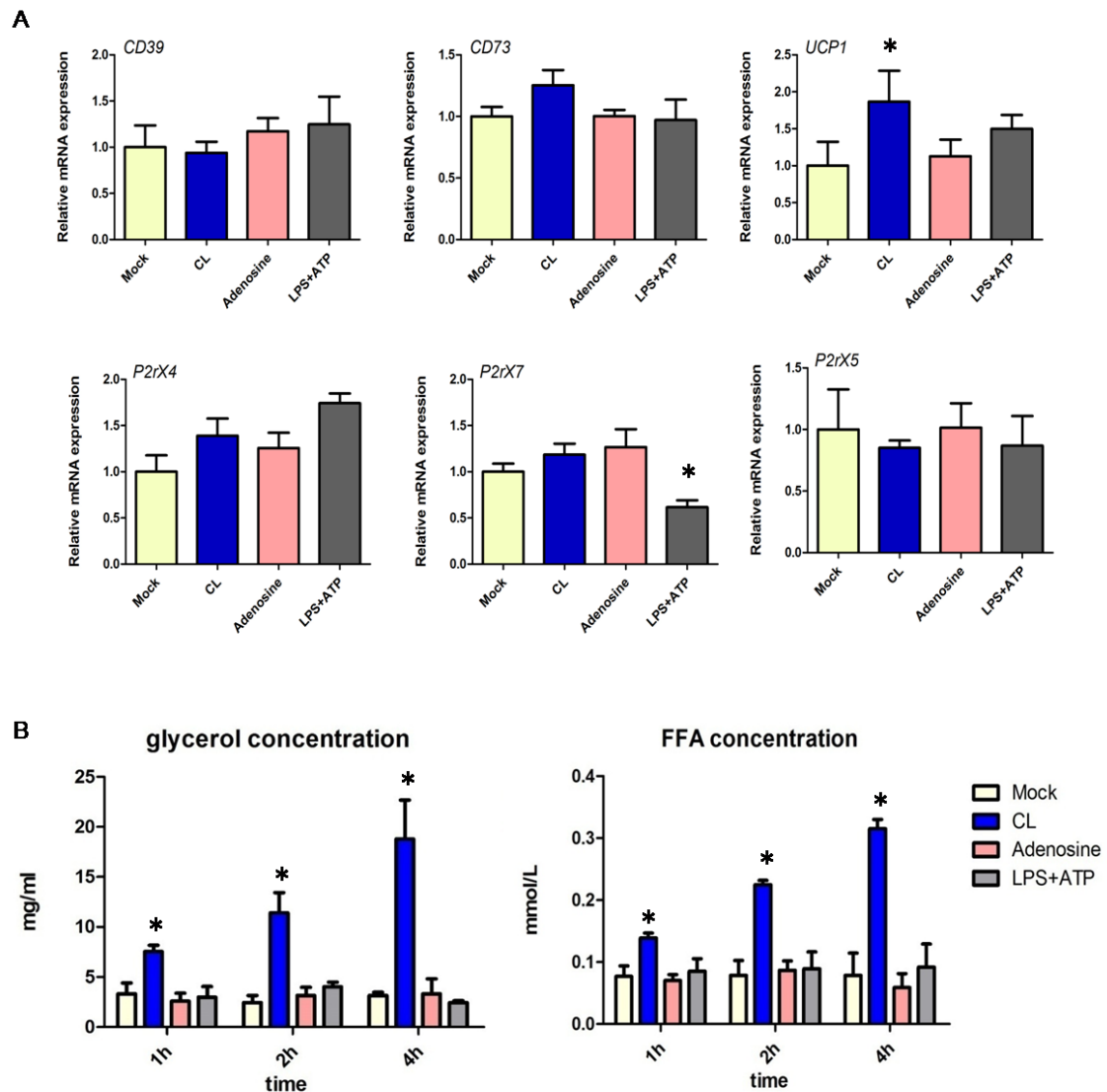
Figure 13. Determination of changes in mRNA expression level and lipolysis in cultured brown adipocytes *in vitro*. Differentiated brown adipocytes were treated with CL (50 nM), adenosine (1 nM), and LPS (0.1 µg/ml) +ATP (100 mM) and cell *supernatants were collected at indicated time points. Expression of CD39, CD73, P2rX7, P2rX4, P2rX5, and Ucp1 were relative to controls. n=3 plate each group. LPS-ATP induced reduction in P2rX7 level. UCP1 level was increased after CL treatment. CL treatment induced significant increase in glycerol and FFA concentrations at 1, 2 and 4h. Data are presented with mean±SEM.*P< 0.05*

P2rX5 expression which could be time- and concentration-dependent. However up to now the role of P2X5 receptor in adipose tissue remains largely unclear.

Macrophages were isolated from mouse bone marrow and treated with CL (50nM), adenosine (1nM) or LPS+ATP (LPS: 0.1μg/ml, ATP: 100mM) for 4 h (Fig.15). Emr1 is a marker for macrophage and was stable in each group under various treatment. After LPS+ATP treatment, significant increase was observed in mRNA expression of IL1b, NLRP3, TNFα and IL6, which indicated that ATP stimulated NLRP3 inflammasome activation and induced the production of a few inflammatory cytokines in the presence of LPS. However, P2rX7 level was decreased after ATP activation. In previous experiment of brown adipocytes I also observed reduced P2rX7 after ATP treatment. This indicates a potential regulation of P2X7 expression by ATP stimulation. One another explanation could be that the inflammation activation attributes mainly to the other cell types in BAT such as endothelial cells. CL, adenosine and ATP did not affect P2rX4 and CD39 levels when compared with controls. CD73 level increased significantly after CL stimulation. P2rX5 mRNA was not detectable in macrophages.
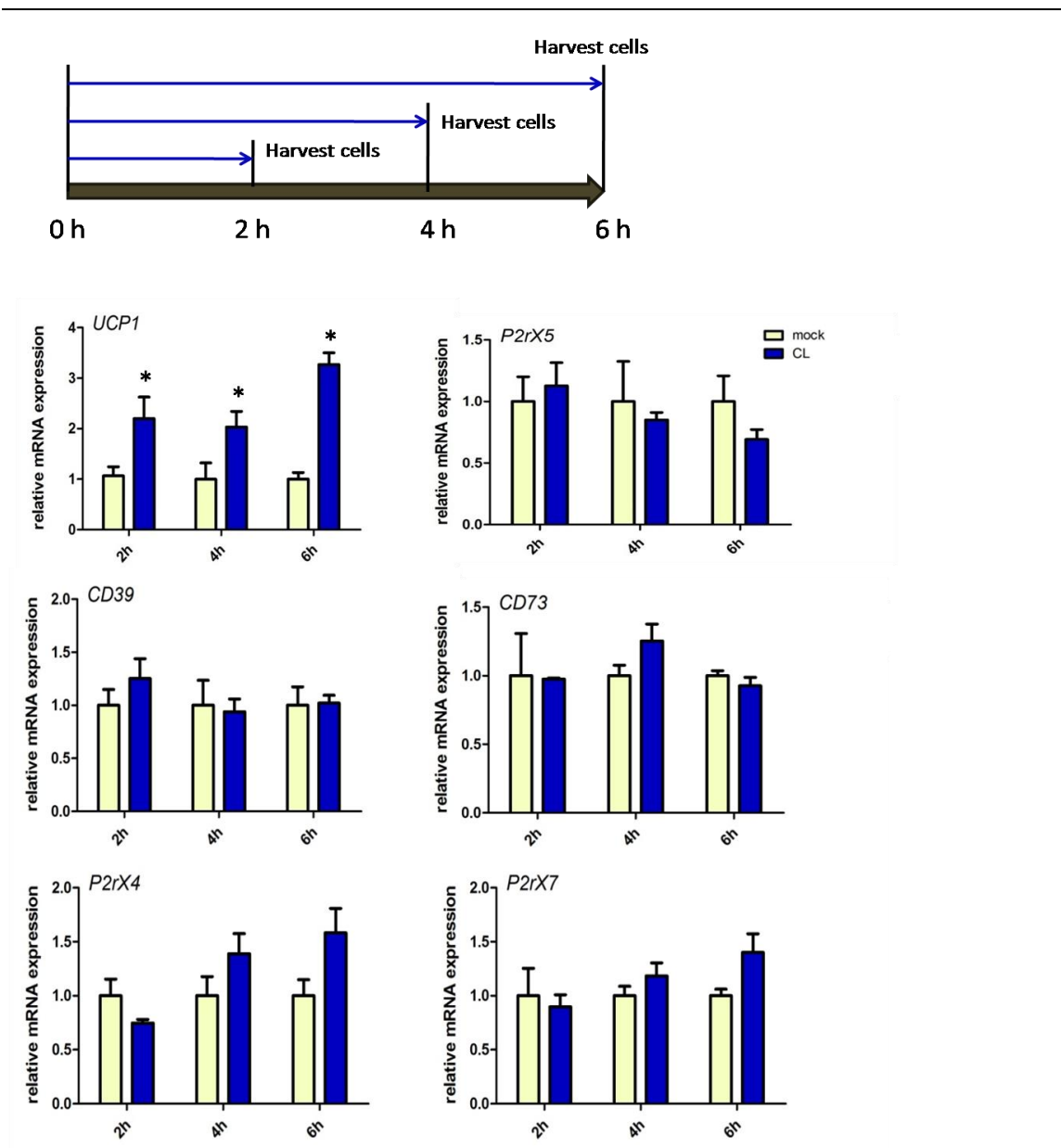
Figure 14. Determination of mRNA expression changes in activated murine brown adipocytes in vitro during time course experiment. *Expression of CD39, CD73, P2rX7, P2rX4, P2rX5, and UCP1 genes were relative to controls (mock 2h). n=3 plates each group. Brown adipocytes were harvested at 2 h, 4 h and 6 h. Data is presented as mean±SEM.*P< 0.05*
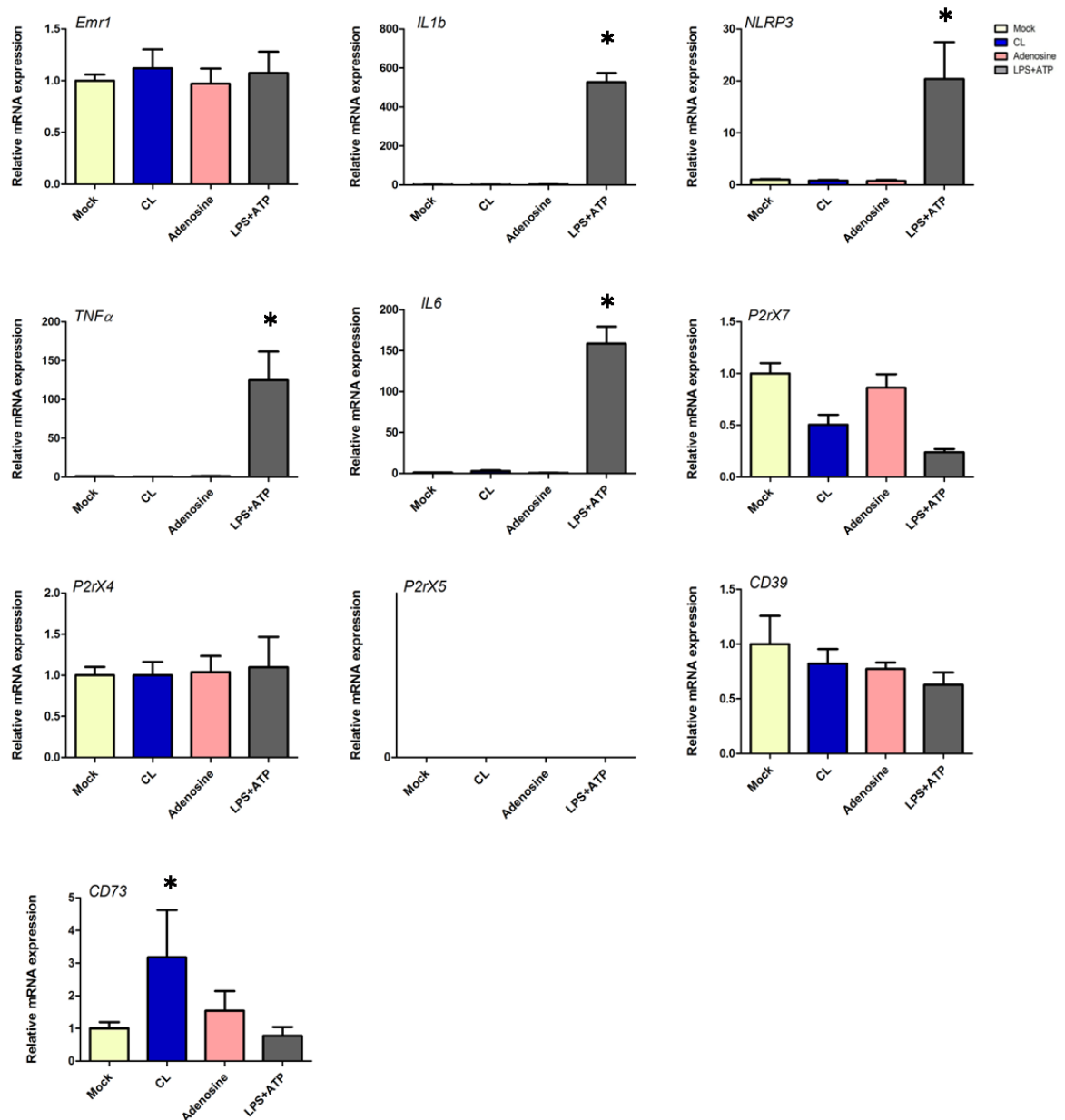
Figure 15. Determination of changes in mRNA expression level in cultured macrophages in vitro. *Macrophages* were treated with CL (50 nM), adenosine (1 nM), and LPS (0.1 µg/ml) +ATP (100 mM). *Expression of Emr1, IL1b, NLRP3, TNFα, IL6, CD39, CD73, P2rX7, P2rX4, P2rX5, and Ucp1 were relative to controls. n=3 plate each group. LPS-ATP induced upregulation of pro-inflammatory and inflammatory genes. CL treatment induced significant increase of CD73. Data is presented with mean±SEM.*P< 0.05*

6. DISSCUSSION

Obesity is associated with insulin resistance in metabolically active organs and tissues such as skeletal muscles, liver and adipose tissue. It has been established that chronic subclinical inflammation in WAT deposits is responsible for the development of insulin resistance in obesity (Uysal et al., 1997). Besides adipocytes, which are the predominant cell type, adipose tissue also contains stromal vascular fraction (SVF) cells including fibroblasts, preadipocytes, endothelial cells and various immune cells such as macrophages, T cells, and B cells. A variety of immune cell types found in adipose tissue not only modulate insulin sensitivity but also regulate other adipose tissue functions. Among them, macrophages play a key role through phagocytosis of dead adipocytes, preventing potentially harmful extracellular lipid accumulation(Weisberg et al., 2003). Endothelial cells in capillaries not only play a role in adipose tissue growth but also participate in variable adipose functions including lipid uptake via glycosylphosphatidylinositol-anchored HDL binding protein 1 (GPIHBP1), which is a binding site for lipoprotein lipase (Sengenes et al., 2007).

Nucleosides and nucleotides are involved in many important functions in physiology and pathophysiology via an extracellular purinergic signaling network, which involves the released ATP, P2X and P2Y family purinergic receptors, ectoenzymes hydrolyzing ATP to adenosine, adenosine receptors and transporters. Extracellular adenosine 5′-triphosphate (ATP) is mainly released from presynaptic neural cells of sympathetic nerves and functions as a classical neurotransmitter. Recent studies indicate ATP can also be released from many other cell types, such as immune, epithelial, stromal cells as well as adipocytes, and participates in modifying a wide range of cell functions, such as lipolysis, lipogenesis, adipogenesis, cell-proliferation and other processes (Burnstock and Novak, 2013). Few studies investigated the contribution of different cell types for the expression of AN receptors and enzymes in adipose tissue. By using MACS cell separation technology, we isolated relatively pure adipocytes, endothelial cells and macrophages from mouse adipose tissue. Our data suggested a role of extracellular purinergic signaling

for interaction between adipocytes, endothelial cells and macrophages in adipose tissue, which may be relevant to the regulation of thermogenic responses. However, further work is needed to understand the precise role of these extracellular purinergic receptors and enzymes for adipose tissue functions including paracrine signaling.

The extracellular ATP binds to P2X and P2Y receptors on cell membrane. P2X receptors are so far divided in seven subtypes (P2X1 to P2X7) according to their different ligand affinity and ion selectivity. Of the P2X family, P2X7 attracts special interest because of its ability to activate inflammasome. Since P2X7 is a key receptor in inflammatory response and widely expressed in immune cells, endocrine cells and adipocytes, it has been considered to participate the pathogenic process of many metabolic disorders like obesity and diabetes. The ATP-gated P2X7 receptor modulates a number of functions in different cell types under physiological and pathological conditions. Aside from its obvious role in immunology, P2X7 was identified to play an important regulatory role in metabolism. Previous study has shown abnormal fat distribution in P2X7 KO mice, revealing an important role for P2X7 in regulating energy and lipid metabolism *in vivo*. In a recent study, P2X7 KO mice displayed decreased energy expenditure and increased RER when kept constant at around 22 °C (Giacovazzo et al., 2018). However, these studies focused on older mice and no gross phenotypic differences were observed in younger mice. (Sun et al., 2012b) (Taylor et al., 2009).

Principally, when exposed to any temperature lower than thermoneutral zone, which is closed to 30°C in mice, animals need extra metabolism to maintain its body temperature homeostasis. The heat can be produced by shivering thermogenesis (acute cold) or non-shivering thermogenesis (prolonged exposure to cold). Here we observed significant increase of energy metabolism induced by cold following reduced environmental temperature from thermoneutral (30 °C) to cold (6 °C) in both P2X7 KO and WT female mice. However, with no altered changes of energy expenditure and input, suggesting a dispensable role for P2X7 in regulating whole-body energy expenditure *in vivo*. Notably,

repeating the energy expenditure experiments in diet-induced obese P2X7 KO male mice, we found similar results.

The P2X7 KO mouse model we used in this study was Pfizer KO mice which was generated by inserting a neomycin insertion in exon 13 of the P2X7 gene and disrupted the P2X7 protein function.(Solle et al., 2001)(Masin et al., 2012)(Bartlett et al., 2014) This strain of mice has been reported to have gender difference in some phenotypes such as bone remodeling (Ke et al., 2003)(Beaucage et al., 2014), that was partly attributed to the interaction between estrogen steroids and P2X7 signaling (Cario-toumaniantz et al., 1998). As mentioned in materials and methods part, the P2X7 KO mouse strain used in my experiment had C57BL/6 background and has been also widely used by other researchers studying relevant function of P2X7 in metabolism. However, it has been demonstrated that the natural mutation P451L underestimates the P2X7 receptor-deficient phenotypes in the wild-type C57BL/6 mouse compared to other mouse strain such as BALB/c which carries 451P SNP (Adriouch et al., 2002) (Young et al., 2006). These studies are mostly restricted in immunology and inflammation, and in the further study it is planned to utilize P2X7 KO mice with BALB/c mouse strain background to determine the role of P2X7 receptor in metabolism.

HFD feeding is known to induce obesity and inflammatory response in adipose tissues. P2X7 was identified as an important role in activating inflammasome as well as inflammatory cytokines secretion through K^+ efflux. P2X7 KO mice were reported to gain more body weight than WT mice upon on long-time chow diet feeding with greater adipose tissue weight (Beaucage et al., 2014). In contrast, another study indicated that P2X7 KO mice and WT mice exhibited similar body weight after chronic exposure to HFD (Sun et al., 2012). Here I found under mild cold condition the HFD feeding induced significant body weight gain in WT and P2X7 KO mice, but without difference between the two cohorts. However, at thermoneutrality P2X7 KO mice exhibited slightly but significant lower body weight gain than WT mice. Combined with the data from metabolic chambers, this may be caused by less body weight gain and less food intake of

P2X7 KO mice. Our results indicate that the ablation of P2X7 does not affect whole body energy expenditure.

P2X7 performs many important functions in different cell populations and thus coordinates complex interactions of inflammatory signaling pathways. Previous study reported that P2X7 was closely related with pancreatic beta cell mass and function (Glas et al., 2009). In this study, P2X7 deficient mice exhibited severe hyperglycemia, glucose intolerance, impaired beta cell mass and function after 12 weeks of a specific high-fat/high-sucrose diet. In my study, 16 weeks of HFD feeding induced hyperglycemia in both P2X7 KO and WT mice, however, they did not show such differences in glucose tolerance. Also, the two cohorts displayed similar plasma insulin, TG and cholesterol levels. Similar results were also observed in another study (Sun et al., 2012), which indicates that P2X7 deficiency did not influence beta -cell–associated diabetic phenotype in obese mice.

It is known that P2X7 receptor is not only presents individual P2X7 homotrimers, but also assembles with P2X4 receptor as heterotrimeric receptors. Within P2X subfamily, P2X7 and P2X4 receptor share the highest similarities: protein sequence homology (48.6% in human sequence and 49.8% in rat), close chromosomal location and overlap in tissue distribution (particularly in immune cells)(Murrell-Lagnado and Qureshi, 2008). P2X4 and P2X7 receptors can also influence the expression of one another. An alveolar epithelial cell line experiment suggests upregulation of P2X4 protein as a compensatory mechanism of P2X7 receptor depletion (Weinhold et al., 2010). Evidence from another study revealed that mRNA levels of P2X4 was significantly decreased in P2X7 KO mice compared with WT mice and P2X7 mRNA expression was down-regulated when P2X4 was genetically ablated. P2X4 protein expression was also reduced in P2X7 KO mice (Craigie et al., 2013). Previous research has also indicated that there is a functional interaction between these two receptors. Prolonged activation of ATP can induce a non-selective pore formation in P2X7 receptor, which are permeable to large molecules. It

was previously thought that this pore formation ability was a characteristic of P2X7 protein. However, new evidence has shown that other P2X receptors can also contribute to pore formation, including P2X2 and P2X4 (Virginio et al., 1999), P2X4, P2X2 and P2X2/3 heterotrimeric complexes, and P2X2/5 heterotrimeric complexes (Khakh et al., 1999).

Some studies indicated that P2X4 was involved in P2X7 mediated inflammatory responses and cell death in macrophages. Co-expression of P2X4 with P2X7 receptor can modulate release of cytokines and suppression of autophagy (Kawano et al., 2012). However, mechanisms for functionally interactions between P2X4 and P2X7 receptors remain largely unknown, and further research in this area is required.

A number of markers have been used to distinguish brown, beige and white adipocytes. These include leptin, Hoxc8 and Hoxc9 for white fat; Tbx1 and Tmem26 for beige fat; and UCP-1, Cidea and Prdm16 for brown fat. New adipocyte cell marker will provide novel insights into adipocyte biology and also facilitate the discovery of new therapeutics targeted into adipose tissue. P2X5 is a newly found marker for mouse brown adipocytes. P2X5 gene and protein expression are significantly higher in brown adipocytes compared to white adipocytes and other cell types. It is also found that P2rX5 expression increases significantly in brown fat and subcutaneous white fat upon chronic cold exposure (Ussar et al., 2014). However the correlation between P2X5 and activation of brown adipocytes is still unknown.

Another notable finding is relevant to P2X5 receptor. Our *in vivo* experiment show that P2rX5 mRNA level is remarkably higher in brown adipocytes than other cell types and cold stimulation induces the increased expression of P2rX5. This is consistent with previous study which identified P2X5 as a novel cell surface marker expressed in brown adipocytes of mice and humans (Ussar et al., 2014). In our *in vitro* experiment P2rX5 remains highly expressed in cultured mature brown adipocytes but β3-ARs stimulation does not induce alterations in expression level of P2rX5, suggesting a mechanism

different from classical adrenergic signaling pathway. Also, a higher P2X5 protein level was observed in BAT compared to other fat depots including WAT in WT mice. To note, obese P2X7 KO mice displayed increased P2X5 protein level compared to WT mice, indicating a potent compensatory mechanism between P2X5 and P2X7 receptors. Thus, future experiment are directed towards illustrating the function of P2X5 receptor in brown adipocytes and its correlation with P2X7 receptor remains to be investigated.

7. SUMMARY

In this study, I determined the expression of purinergic receptors (P2X4, P2X7, and P2X5) and enzymes (CD39, CD73) in isolated adipocytes, endothelial cells, and macrophages in WAT and BAT under mild cold (22 °C) and cold (6 °C) conditions. My results show that the expression of AN receptor P2X7 is increased in isolated macrophage cell population in WAT and BAT upon acute cold exposure. In order to determine the physiological and pathophysiological effect of P2X7 in vivo, I used P2X7 knock out mouse. My results indicate that deficiency of P2X7 is dispensable for energy expenditure and food intake at thermoneutrality and acute cold exposure compared to wild-type mice. Moreover, despite moderate effect on inflammation in gonadal white adipose tissue, P2X7 deficiency does not alter diet-induced obesity, insulin resistance and hyperglycemia associated with high-fat diet feeding.

ZUSAMMENFASSUNG (deutsch)

In dieser Studie haben wir die Expression von purinergen Rezeptoren (P2X4, P2X7 und P2X5) und Enzymen (CD39, CD73) in isolierten Adipozyten, Endothelzellen und Makrophagen in WAT und BAT bei milder Kälte (22 ° C) und Kälte (6 ° C) Bedingungen untersucht. Meine Ergebnisse zeigen, dass die Expression des AN-Rezeptors P2X7 in der Population der isolierten Makrophagen in WAT und BAT bei akuter Kälteexposition erhöht ist. Um die physiologische und pathophysiologische Wirkung von P2X7 in vivo zu bestimmen, habe Ich P2X7-Knock-Out-Mäuse verwendet. Meine Ergebnisse zeigen, dass ein Mangel an P2X7 im Vergleich zu Wildtyp-Mäusen für den Energieverbrauch und die Nahrungsaufnahme bei Thermoneutralität und akuter Kälteexposition überflüssig ist. Trotz eines mäßigen Effekts auf Entzündungsprozesse im gonadalen weißen-Fettgewebe, hat die P2X7-Defizienz keinen Einfluss auf die durch Hochfettdiät-induzierte Adipositas, Insulinresistenz und Hyperglykämie.

8. REFERENCES

Adinolfi, E., Cirillo, M., Woltersdorf, R., Falzoni, S., Chiozzi, P., Pellegatti, P., Callegari, M.G., Sandona, D., Markwardt, F., Schmalzing, G., et al. (2010). Trophic activity of a naturally occurring truncated isoform of the P2X7 receptor. FASEB J. *24*, 3393–3404.

Adriouch, S., Dox, C., Welge, V., Seman, M., Koch-Nolte, F., and Haag, F. (2002). Cutting Edge: A Natural P451L Mutation in the Cytoplasmic Domain Impairs the Function of the Mouse P2X7 Receptor. J. Immunol. *169*, 4108–4112.

Adriouch S, Dubberke G, Diessenbacher P, Rassendren F, Seman M, Haag F, K.-N.F. (2005). Probing the expression and function of the P2X7 purinoceptor with antibodies raised by genetic immunization. Cell Immunol *236*, 72–77.

Ali, A.T., Hochfeld, W.E., Myburgh, R., and Pepper, M.S. (2013). Adipocyte and adipogenesis. Eur J Cell Biol *92*, 229–236.

Antonio, L.S., Stewart, a. P., Xu, X.J., Varanda, W. a., Murrell-Lagnado, R.D., and Edwardson, J.M. (2011). P2X4 receptors interact with both P2X2 and P2X7 receptors in the form of homotrimers. Br. J. Pharmacol. *163*, 1069–1077.

Antonioli, L., Blandizzi, C., Pacher, P., and Haskó, G. (2013). Immunity, inflammation and cancer: A leading role for adenosine. Nat. Rev. Cancer *13*, 842–857.

Baljit S. Khakh and R. Alan North (2014). Neuromodulation by extracellular ATP and P2X receptors in the CNS. Neuron *76*, 51–69.

Bartelt, A., and Heeren, J. (2014). Adipose tissue browning and metabolic health. Nat Rev Endocrinol *10*, 24–36.

Bartlett, R., Stokes, L., and Sluyter, R. (2014). The P2X7 receptor channel: recent developments and the use of P2X7 antagonists in models of disease. Pharmacol Rev *66*, 638–675.

Bartness, T.J., Liu, Y., Shrestha, Y.B., and Ryu, V. (2014). Neural innervation of white adipose tissue and the control of lipolysis. Front Neuroendocr. *35*, 473–493.

Bolsoni-Lopes, A., and Alonso-Vale, M.I.C. (2015). Lipolysis and lipases in white adipose tissue – An update. Arch. Endocrinol. Metab. *59*, 335–342.

Boucher, J., Masri, B., Daviaud, D., Gesta, S., Guigne, C., Mazzucotelli, A., Castan-Laurell, I., Tack, I., Knibiehler, B., Carpene, C., et al. (2005). Apelin, a newly identified adipokine up-regulated by insulin and obesity. Endocrinology *146*, 1764–1771.

Boumechache, M., Masin, M., Edwardson, J.M., Górecki, D., and Murrell-Lagnado, R. (2009). Analysis of assembly and trafficking of native P2X4 and P2X7 receptor complexes in rodent immune cells. J. Biol. Chem. *284*, 13446–13454.

Brychta, R.J., and Chen, K.Y. (2017). Cold-induced thermogenesis in humans. Eur J Clin Nutr *71*, 345–352.

Buell GN, Talabot F, Gos A, Lorenz J, Lai E, Morris MA, A.S. (1998). Gene structure and chromosomal localization of the human P2X7 receptor. Recept. Channels *5*, 347–354.

Burnstock, G. (2006). Purinergic signalling. Br. J. Pharmacol. *147*, 172–181.

Burnstock, G. (2014). Purinergic signalling: From discovery to current developments. Exp. Physiol. *99*, 16–34.

Burnstock, G., and Novak, I. (2013). Purinergic signalling and diabetes. Purinergic Signal *9*, 307–324.

Cannon, B. (2004). Brown Adipose Tissue: Function and Physiological Significance. Physiol. Rev. *84*, 277–359.

Cannon, B., and Nedergaard, J. (2004). Brown adipose tissue: function and physiological significance. Physiol Rev *84*, 277–359.

Cannon, B., and Nedergaard, J. (2011). Nonshivering thermogenesis and its adequate measurement in metabolic studies. J. Exp. Biol. *214*, 242–253.

Cario-toumaniantz, C., Loirand, G., Ferrier, L., Pacaud, P., Pharmacologie, I. De, Upr, C., and Antipolis, S. (1998). Rapid Report Non-genomic inhibition of human P2X 7 purinoceptor by 17â _ oestradiol. 659–666.

Cawthorn, W.P., and Sethi, J.K. (2008). TNF-alpha and adipocyte biology. FEBS Lett. *582*, 117–131.

Chaumont, S., and Khakh, B.S. (2008). Patch-clamp coordinated spectroscopy shows P2X2 receptor permeability dynamics require cytosolic domain rearrangements but not Panx-1 channels. Proc. Natl. Acad. Sci. *105*, 12063–12068.

Cinti, S. (2001). The adipose organ: morphological perspectives of adipose tissues. Proc. Nutr. Soc. *60*, 319–328.

Coddou, C., Stojilkovic, S.S., and Huidobro-Toro, J.P. (2011). Allosteric modulation of ATP-gated P2X receptor channels. Rev. Neurosci. *22*, 335–354.

Combs, T.P., Pajvani, U.B., Berg, A.H., Lin, Y., Jelicks, L.A., Laplante, M., Nawrocki, A.R., Rajala, M.W., Parlow, A.F., Cheeseboro, L., et al. (2004). A transgenic mouse with a deletion in the collagenous domain of adiponectin displays elevated circulating adiponectin and improved insulin sensitivity. Endocrinology *145*, 367–383.

Commins, S.P., Watson, P.M., Frampton, I.C., and Gettys, T.W. (2001). Leptin selectively reduces white adipose tissue in mice via a UCP1-dependent mechanism in brown adipose tissue. Am J Physiol Endocrinol Metab *280*, E372–E377.

Compan, V., Ulmann, L., Stelmashenko, O., Chemin, J., Chaumont, S., and Rassendren, F. (2012). P2X2 and P2X5 Subunits Define a New Heteromeric Receptor with P2X7-Like Properties. J. Neurosci. *32*, 4284–4296.

Cousin, B., Agou, K., Leturque, A., Ferre, P., Girard, J., and Penicaud, L. (1992). Molecular and metabolic changes in white adipose tissue of the rat during development of ventromedial hypothalamic obesity. Eur J Biochem *207*, 377–382.

Craigie, E., Birch, R.E., Unwin, R.J., and Wildman, S.S. (2013). The relationship between P2X4 and P2X7: A physiologically important interaction? Front. Physiol. *4 AUG*, 1–6.

Denlinger, L.C., Fisette, P.L., Sommer, J. a., Watters, J.J., Prabhu, U., Dubyak, G.R., Proctor, R. a., and Bertics, P.J. (2001). Cutting Edge: The Nucleotide Receptor P2X7 Contains Multiple Protein- and Lipid-Interaction Motifs Including a Potential Binding Site for Bacterial Lipopolysaccharide. J. Immunol. *167*, 1871–1876.

Dimitriadis, G., Mitrou, P., Lambadiari, V., Maratou, E., and Raptis, S.A. (2011). Insulin effects in muscle and adipose tissue. Diabetes Res Clin Pr. *93 Suppl 1*, S52–S59.

Eissing, L., Scherer, T., Todter, K., Knippschild, U., Greve, J.W., Buurman, W.A., Pinnschmidt, H.O., Rensen, S.S., Wolf, A.M., Bartelt, A., et al. (2013). De novo lipogenesis in human fat and liver is linked to ChREBP-beta and metabolic health. Nat Commun *4*, 1528.

Farmer, S.R. (2006). Transcriptional control of adipocyte formation. Cell Metab *4*, 263–273.

Fasshauer, M., and Bluher, M. (2015). Adipokines in health and disease. Trends Pharmacol Sci *36*, 461–470.

Feldmann, H.M., Golozoubova, V., Cannon, B., and Nedergaard, J. (2009). UCP1 ablation induces obesity and abolishes diet-induced thermogenesis in mice exempt from thermal stress by living at thermoneutrality. Cell Metab *9*, 203–209.

Ferre, P., and Foufelle, F. (2007). SREBP-1c transcription factor and lipid homeostasis: clinical perspective. Horm Res *68*, 72–82.

Fredriksson, R. (2003). The G-Protein-Coupled Receptors in the Human Genome Form Five Main Families. Phylogenetic Analysis, Paralogon Groups, and Fingerprints. Mol. Pharmacol. *63*, 1256–1272.

Frontini, A., and Cinti, S. (2010). Distribution and development of brown adipocytes in the murine and human adipose organ. Cell Metab *11*, 253–256.

Generation, I. (1990). The Adenosine / Neutrophil Paradox Resolved : Human Neutrophils Possess Both A1 and A2 Receptors that Promote. *85*, 1150–1157.

Giacovazzo, G., Apolloni, S., and Coccurello, R. (2018). Loss of P2X7 receptor function dampens whole body energy expenditure and fatty acid oxidation. Purinergic Signal.

Glas, R., Sauter, N.S., Schulthess, F.T., Shu, L., Oberholzer, J., and Maedler, K. (2009). Purinergic P2X7 receptors regulate secretion of interleukin-1 receptor antagonist and beta cell function and survival. Diabetologia *52*, 1579–1588.

Gnad, T., Scheibler, S., Kugelgen, I. Von, Scheele, C., Kilic, A., Glode, A., Hoffmann, L.S., Reverte-Salisa, L., Horn, P., Mutlu, S., et al. (2014). Adenosine activates brown adipose tissue and recruits beige adipocytes via A2Areceptors. Nature *516*, 395–399.

Gombault, A., Baron, L., and Couillin, I. (2012). ATP release and purinergic signaling in NLRP3 inflammasome activation. Front. Immunol. *3*, 1–6.

Griggio, M.A. (1982). The participation of shivering and nonshivering thermogenesis in warm and cold-acclimated rats. Comp Biochem Physiol A Comp Physiol *73*, 481–484.

Grujic, D., Susulic, V.S., Harper, M., Himms-hagen, J., Cunningham, B. a, Corkey, B.E., and Lowell, B.B. (1997). Beta3-adrenergic receptors on white and brown adipocytes mediate beta3-selective agonist-induced effects on energy expenditure, insulin secretion, and food intake. J Biol Chem *272*, 17686–17693.

Gu, B.J., Zhang, W.Y., Bendall, L.J., Chessell, I.P., Buell, G.N., and Wiley, and J.S. (2000). Expression of P2X7 purinoceptors on human lymphocytes and monocytes : evidence for nonfunctional P2X7 receptors Expression of P2X 7 purinoceptors on human lymphocytes and monocytes : evidence for nonfunctional P2X 7 receptors. Am J Physiol Cell Physiol *279*, 1189–1197.

He, Y., Hara, H., and Núñez, G. (2016). Mechanism and Regulation of NLRP3 Inflammasome Activation. Trends Biochem. Sci. *41*, 1012–1021.

Himms-Hagen, J. (1995). Does thermoregulatory feeding occur in newborn infants? A novel view of the role   of brown adipose tissue thermogenesis in control of food intake. Obes. Res. *3*, 361–369.

Hoffstedt, J., Arvidsson, E., Sjolin, E., Wahlen, K., and Arner, P. (2004). Adipose tissue adiponectin production and adiponectin serum concentration in human obesity and insulin resistance. J Clin Endocrinol Metab *89*, 1391–1396.

Horenstein, A.L., Chillemi, A., Zaccarello, G., Bruzzone, S., Quarona, V., Zito, A., Serra, S., and Malavasi, F. (2013). A CD38/CD203A/CD73 ectoenzymatic pathway independent of CD39 drives a novel adenosinergic loop in human T lymphocytes. Oncoimmunology *2*, 1–14.

Hui, X., Lam, K.S., Vanhoutte, P.M., and Xu, A. (2012). Adiponectin and cardiovascular health: an update. Br J Pharmacol *165*, 574–590.

Hui, X., Gu, P., Zhang, J., Nie, T., Pan, Y., Wu, D., Feng, T., Zhong, C., Wang, Y., Lam, K.S., et al. (2015). Adiponectin Enhances Cold-Induced Browning of Subcutaneous Adipose Tissue via Promoting M2 Macrophage Proliferation. Cell Metab *22*, 279–290.

Iozzo, P. (2011). Myocardial, perivascular, and epicardial fat. Diabetes Care *34 Suppl 2*, S371–S379.

Jacobson, K. a., and Gao, Z.G. (2006). Adenosine receptors as therapeutic targets. Nat. Rev. Drug Discov. *5*, 247–264.

Jacobson, K. a., Balasubramanian, R., Deflorian, F., and Gao, Z.G. (2012). G protein-coupled adenosine (P1) and P2Y receptors: Ligand design and receptor interactions. Purinergic Signal. *8*, 419–436.

Jeremic, N., Chaturvedi, P., and Tyagi, S.C. (2017). Browning of White Fat: Novel Insight Into Factors, Mechanisms, and Therapeutics. J Cell Physiol *232*, 61–68.

Jørgensen, N.R., Husted, L.B., Skarratt, K.K., Stokes, L., Tofteng, C.L., Kvist, T., Jensen, J.E.B., Eiken, P., Brixen, K., Fuller, S., et al. (2012). Single-nucleotide polymorphisms in the P2X7 receptor gene are associated with post-menopausal bone loss and vertebral fractures. Eur. J. Hum. Genet. *20*, 675–681.

Kanda, H., Tateya, S., Tamori, Y., Kotani, K., Hiasa, K., Kitazawa, R., Kitazawa, S., Miyachi, H., Maeda, S., Egashira, K., et al. (2006). MCP-1 contributes to macrophage infiltration into adipose tissue, insulin resistance, and hepatic steatosis in obesity. J Clin Invest *116*, 1494–1505.

Kawano, A., Tsukimoto, M., Mori, D., Noguchi, T., Harada, H., Takenouchi, T., Kitani, H., and Kojima, S. (2012). Regulation of P2X7-dependent inflammatory functions by P2X4 receptor in mouse macrophages. Biochem. Biophys. Res. Commun. *420*, 102–107.

Kershaw, E.E., and Flier, J.S. (2004). Adipose tissue as an endocrine organ. J Clin Endocrinol Metab *89*, 2548–2556.

Kersten, S. (2001). Mechanisms of nutritional and hormonal regulation of lipogenesis. EMBO Rep *2*, 282–286.

Kersten, S. (2014). Physiological regulation of lipoprotein lipase. Biochim Biophys Acta *1841*, 919–933.

Khakh, B.S., and Alan North, R. (2006). P2X receptors as cell-surface ATP sensors in health and disease. Nature *442*, 527–532.

Khakh, B.S., Bao, X.R., Labarca, C., and Lester, H. a. (1999). Neuronal P2X transmitter-gated cation channels change their ion selectivity in seconds. Nat. Neurosci. *2*, 322–330.

Kurashima, Y., Amiya, T., Nochi, T., Fujisawa, K., Haraguchi, T., Iba, H., Tsutsui, H., Sato, S., Nakajima, S., Iijima, H., et al. (2012). Extracellular ATP mediates mast cell-dependent intestinal inflammation through P2X7 purinoceptors. Nat. Commun. *3*, 1012–1034.

Lass, A., Zimmermann, R., Oberer, M., and Zechner, R. (2011). Lipolysis - a highly regulated multi-enzyme complex mediates the catabolism of cellular fat stores. Prog Lipid Res *50*, 14–27.

Lean, M.E. (1989). Brown adipose tissue in humans. Proc Nutr Soc *48*, 243–256.

Lefterova, M.I., and Lazar, M. a. (2009a). New developments in adipogenesis. Trends Endocrinol. Metab. *20*, 107–114.

Lefterova, M.I., and Lazar, M.A. (2009b). New developments in adipogenesis. Trends Endocrinol Metab *20*, 107–114.

Lidell, M.E., Betz, M.J., Dahlqvist Leinhard, O., Heglind, M., Elander, L., Slawik, M., Mussack, T., Nilsson, D., Romu, T., Nuutila, P., et al. (2013). Evidence for two types of brown adipose tissue in humans. Nat. Med. *19*, 631–634.

Lodhi, I.J., Yin, L., Jensen-urstad, A.P.L., Funai, K., Coleman, T., Baird, H., Ramahi, M.K. El, Razani, B., Song, H., Fu-hsu, F., et al. (2013). Inhibiting Adipose Tissue Lipogenesis Reprograms Thermogenesis and PPARγ Activation to Decrease Diet-induced Obesity. Cell Metab. *16*, 189–201.

Masaki, T., Chiba, S., Yasuda, T., Tsubone, T., Kakuma, T., Shimomura, I., Funahashi, T., Matsuzawa, Y., and Yoshimatsu, H. (2003). Peripheral, but not central, administration of adiponectin reduces visceral adiposity and upregulates the expression of uncoupling protein in agouti yellow (Ay/a) obese mice. Diabetes *52*, 2266–2273.

Masin, M., Young, C., Lim, K., Barnes, S.J., Xu, X.J., Marschall, V., Brutkowski, W., Mooney, E.R., Gorecki, D.C., and Murrell-Lagnado, R. (2012). Expression, assembly and function of novel C-terminal truncated variants of the mouse P2X7 receptor: re-evaluation of P2X7 knockouts. Br J Pharmacol *165*, 978–993.

Morrison, S.F. (2016). Central neural control of thermoregulation and brown adipose tissue. Aut. Neurosci *196*, 14–24.

Murrell-Lagnado, R.D., and Qureshi, O.S. (2008). Assembly and trafficking of P2X purinergic receptors (Review). Mol. Membr. Biol. *25*, 321–331.

Nedergaard, J., and Cannon, B. (2014). The browning of white adipose tissue: Some burning issues. Cell Metab. *20*, 396–407.

Nedergaard, J., Bengtsson, T., and Cannon, B. (2007). Unexpected evidence for active brown adipose tissue in adult humans. Am J Physiol Endocrinol Metab *293*, E444–E452.

Nelson, E.E., and Guyer, A.E. (2012). NIH Public Access. *1*, 233–245.

North, R.A. (2016). P2X receptors. Philos Trans R Soc L. B Biol Sci *371*.

Nuutila, P. (2015). Brown adipose tissue in humans. Ann Med *47*, 122.

Petrovic, N., Walden, T.B., Shabalina, I.G., Timmons, J.A., Cannon, B., and Nedergaard, J. (2010). Chronic peroxisome proliferator-activated receptor gamma (PPARgamma) activation of epididymally derived white adipocyte cultures reveals a population of thermogenically competent, UCP1-containing adipocytes molecularly distinct from classic brown adipocyt. J Biol Chem *285*, 7153–7164.

Picard, F., Naimi, N., Richard, D., and Deshaies, Y. (1999). Response of adipose tissue lipoprotein lipase to the cephalic phase of insulin secretion. Diabetes *48*, 452–459.

Rassendren, F., Buell, G.N., Virginio, C., Collo, G., North, R. a, and Surprenant, A. (1997). The Permeabilizing ATP Receptor, P2X7. J. Biol. Chem. *272*, 5482–5486.

Rose, J.B., and Coe, I.R. (2008). Physiology of Nucleoside Transporters : Physiology *23*, 41–48.

Rosen, E.D., and Spiegelman, B.M. (2014). What we talk about when we talk about fat. Cell *156*, 20–44.

Rosen, E.D., Sarraf, P., Troy, A.E., Bradwin, G., Moore, K., Milstone, D.S., Spiegelman, B.M., and Mortensen, R.M. (1999). PPAR gamma is required for the differentiation of adipose tissue in vivo and in vitro. Mol Cell *4*, 611–617.

Rosen, E.D., Hsu, C.H., Wang, X., Sakai, S., Freeman, M.W., Gonzalez, F.J., and Spiegelman, B.M. (2002). C/EBPalpha induces adipogenesis through PPARgamma: a unified pathway. Genes Dev *16*, 22–26.

Rothwell, N.J., and Stock, M.J. (1997). A role for brown adipose tissue in diet-induced thermogenesis. Obes Res *5*, 650–656.

Sacks, H., and Symonds, M.E. (2013). Anatomical locations of human brown adipose tissue: functional relevance and implications in obesity and type 2 diabetes. Diabetes *62*, 1783–1790.

Schilling, W.P., Sinkins, W.G., and Estacion, M. (1999). Maitotoxin activates a nonselective cation channel and a P2Z / P2X 7 -like cytolytic pore in human skin fibroblasts Maitotoxin activates a nonselective cation channel and a P2Z / P2X 7 -like cytolytic pore in human skin fibroblasts. Am J Physiol *277*, C755–C765.

Schmidt, S., Jørgensen, M., Chen, Y., and Nielsen, R. (2011). BMC Genomics | Full text | Cross species comparison of C/EBPalpha and PPARgamma profiles in mouse and human adipocytes reveals interdependent retention of binding sites. Bmc ….

Sengenes, C., Miranville, A., Lolmede, K., Curat, C.A., and Bouloumie, A. (2007). The role of endothelial cells in inflamed adipose tissue. J. Intern. Med. *262*, 415–421.

Smart, M.L., Gu, B., Panchal, R.G., Wiley, J., Cromer, B., Williams, D. a., and Petrou, S. (2003). P2X7 receptor cell surface expression and cytolytic pore formation are regulated by a distal C-terminal region. J. Biol. Chem. *278*, 8853–8860.

Sun, S., Xia, S., Ji, Y., Kersten, S., and Qi, L. (2012a). The ATP-P2X7signaling axis is dispensable for obesity-associated inflammasome activation in adipose tissue. Diabetes *61*, 1471–1478.

Sun, S., Xia, S., Ji, Y., Kersten, S., and Qi, L. (2012b). The ATP-P2X7 signaling axis is dispensable for obesity-associated inflammasome activation in adipose tissue. Diabetes *61*, 1471–1478.

Surprenant, A., and North, R.A. (2009). Signaling at Purinergic P2X Receptors. Annu. Rev. Physiol. *71*, 333–359.

Tansey, E.A., and Johnson, C.D. (2015). Recent advances in thermoregulation. Adv Physiol Educ *39*, 139–148.

Taylor, S.R.J., Gonzalez-Begne, M., Sojka, D.K., Richardson, J.C., Sheardown, S. a., Harrison, S.M., Pusey, C.D., Tam, F.W.K., and Elliott, J.I. (2009). Lymphocytes from P2X7-deficient mice exhibit enhanced P2X7 responses. J. Leukoc. Biol. *85*, 978–986.

Tomas, E., Tsao, T.S., Saha, A.K., Murrey, H.E., Zhang Cc, C., Itani, S.I., Lodish, H.F., and Ruderman, N.B. (2002). Enhanced muscle fat oxidation and glucose transport by ACRP30 globular domain: acetyl-CoA carboxylase inhibition and AMP-activated protein kinase activation. Proc Natl Acad Sci U S A *99*, 16309–16313.

Tontonoz, P., Graves, R.A., Budavari, A.I., Erdjument-Bromage, H., Lui, M., Hu, E., Tempst, P., and Spiegelman, B.M. (1994a). Adipocyte-specific transcription factor ARF6 is a

heterodimeric complex of two nuclear hormone receptors, PPAR gamma and RXR alpha. Nucleic Acids Res *22*, 5628–5634.

Tontonoz, P., Hu, E., and Spiegelman, B.M. (1994b). Stimulation of adipogenesis in fibroblasts by PPAR gamma 2, a lipid-activated transcription factor. Cell *79*, 1147–1156.

Tozzi, M., and Novak, I. (2017). Purinergic Receptors in Adipose Tissue As Potential Targets in Metabolic Disorders. Front. Pharmacol. *8*.

Ussar, S., Lee, K.Y., Dankel, S.N., Boucher, J., Haering, M.F., Kleinridders, A., Thomou, T., Xue, R., Macotela, Y., Cypess, A.M., et al. (2014). ASC-1, PAT2, and P2RX5 are cell surface markers for white, beige, and brown adipocytes. Sci. Transl. Med. *6*.

Uysal, K.T., Wiesbrock, S.M., Marino, M.W., and Hotamisligil, G.S. (1997). Protection from obesity-induced insulin resistance in mice lacking TNF-alpha function. Nature *389*, 610–614.

Vandanmagsar, B., Youm, Y., Ravussin, A., Galgani, J.E., Stadler, K., Mynatt, R.L., Ravussin, E., Stephens, J.M., and Dixit, V.D. (2011). The NLRP3 inflammasome instigates obesity-induced inflammation and insulin resistance. Nat Med *17*, 179–188.

Vidal-Puig, A., Jimenez-Linan, M., Lowell, B.B., Hamann, A., Hu, E., Spiegelman, B., Flier, J.S., and Moller, D.E. (1996). Regulation of PPAR gamma gene expression by nutrition and obesity in rodents. J Clin Invest *97*, 2553–2561.

Virginio, C., MacKenzie, a., Rassendren, F. a., North, R. a., and Surprenant, a. (1999). Pore dilation of neuronal P2X receptor channels. Nat. Neurosci. *2*, 315–321.

Weber, F.C., Esser, P.R., Muller, T., Ganesan, J., Pellegatti, P., Simon, M.M., Zeiser, R., Idzko, M., Jakob, T., and Martin, S.F. (2010). Lack of the purinergic receptor P2X(7) results in resistance to contact hypersensitivity. J Exp Med *207*, 2609–2619.

Weinhold, K., Krause-Buchholz, U., Rödel, G., Kasper, M., and Barth, K. (2010). Interaction and interrelation of P2X7 and P2X4 receptor complexes in mouse lung epithelial cells. Cell. Mol. Life Sci. *67*, 2631–2642.

Weisberg, S.P., McCann, D., Desai, M., Rosenbaum, M., Leibel, R.L., and Ferrante Jr., A.W. (2003). Obesity is associated with macrophage accumulation in adipose tissue. J Clin Invest *112*, 1796–1808.

Wronska, A., and Kmiec, Z. (2012). Structural and biochemical characteristics of various white adipose tissue depots. Acta Physiol *205*, 194–208.

Young, M.T., Pelegrin, P., and Surprenant, a. (2006). Identification of Thr 283 as a key determinant of P2X 7 receptor function. Br. J. Pharmacol. *149*, 261–268.

Young, P., Wilson, S., and Arch, J.R. (1984). Prolonged beta-adrenoceptor stimulation increases the amount of GDP-binding protein in brown adipose tissue mitochondria. Life Sci *34*, 1111–1117.

Zechner, R., Kienesberger, P.C., Haemmerle, G., Zimmermann, R., and Lass, A. (2009). Adipose triglyceride lipase and the lipolytic catabolism of cellular fat stores. J Lipid Res *50*, 3–21.

Zhang, Y., Proenca, R., Maffei, M., Barone, M., Leopold, L., and Friedman, J.M. (1994). Positional cloning of the mouse obese gene and its human homologue. Nature *372*, 425–432.

Zhao, H., Bo, C., Kang, Y., and Li, H. (2017). What else can CD39 tell us? Front. Immunol. *8*, 1–10.

Zimmermann, H., Zebisch, M., and Strater, N. (2012). Cellular function and molecular structure of ecto-nucleotidases. Purinergic Signal *8*, 437–502.

9. LIST OF ABBREVIATIONS

ACC   Acetyl-CoA Carboxylase

AMPK   AMP-Activated Protein Kinase

ATP   Adenosine 5'-Triphosphate

BAT   Brown Adipose Tissue

C/EBP   CCAAT/Enhancer-Binding Proteins

CoA   Coenzyme A

DIO   Diet-Induced Obesity

DNL   *De novo* lipogenesis

eN   ecto-5'-Nucleotidase

E-NTPDase   EctoNucleoside Triphosphate Diphosphohydrolase

FACS   Fluorescence-Activated Cell Sorting

FAS   Fatty Acid Synthase

FDG   Fluorodeoxyglucose

FFA   Free Fatty Acid

gWAT   gonadal WAT

GPCR   G-Protein-Coupled Receptor

GPIHBP1   Glycosylphosphatidylinositol-anchored HDL Binding Protein 1

iBAT   interscapular BAT

iWAT   inguinal WAT

LPL   Lipoprotein lipase

LPS   Lipopolysaccharide

MACS   Magnetic Activated Cell Sorting

MAPK   Mitogen-Activated Protein Kinases

MSC   Mesenchymal Stem Cells

NAD   Nicotinamide Adenine Dinucleotide

NE   Norepinephrine

NLR   Nucleotide-binding oligomerization domain-Like Receptors

PAMP   Pathogen-Associated Molecular Pattern

PET   Positron Emission Tomography

PPAR-γ   Peroxisome Proliferator-Activated Receptor gamma

RER   Respiratory Exchange Ratio

ROS   Reactive Oxygen Species

subWAT   subcutaneous WAT

SNP   Single Nucleotide Polymorphism

SREBP1c   Sterol Regulatory Element-Binding Protein 1c

SVF   Stromal Vascular Fraction

TG   Triglyceride

TLR   Toll-Like Receptors

TNF-a   Tumor Necrosis Factor-alpha

UCP-1   Uncoupling Protein-1

VLDL   Very Low-Density Lipoprotein

WAT   White Adipose Tissue

10. ACKNOWLEDGEMENTS

First, I would like to express my sincere thanks to my supervisor Prof. Jörg Heeren for his valuable guidance, direction and encouragement. I would like to give special thanks to Dr. Manju Kumari for technological aids and timely suggestions throughout my project. To my fellow labmates in Heeren Lab, thank you all. In particular, I would thank Dr. Markus Heine and Dr. Alexander Fisher for valuable assistance, Ioannis Evangelakos for encouragement and cooperation during my experiments. My grateful thanks are also extended to Sandra Ehret, Birgit Henkel, and Walter Tauscher who gave me access to the laboratory and research facilities.

I would also like to thank all my friends for companionship and help through the process of researching and writing this thesis. Finally I must express my very profound gratitude to my family for unconditional support through my years of study abroad. This accomplishment would not have been possible without them. Thank you.

11. CURRICULUM VITAE

Persönliche Daten					
Name	**Tian Tian**	Geschlecht	**weiblich**	Geburtsdatum	**20. 08. 1993**
Geburtsort	**Provinz Anhui, VR China**	Familienstand	**ledig**	Staatsangehörigkeit	**chinesisch**
Anschrift	**Fibiger Strasse 163**			PLZ	**22419**
E-Mail	**tiantiantian2014@163.com**			Telefon	**+4917624641634**
Ausbildung					
09. 1998	**06. 2003**	**Zentrale Grundschule, Gemeinde Erba, Stadt Wuhu, Provinz Anhui**			
09. 2003	**06. 2006**	**Erba-Mittelstufe, Stadt Wuhu, Provinz Anhui**			
09. 2006	**06. 2009**	**Wuwei-Oberstufe, Provinz Anhui**			
09. 2009	**06. 2014**	**Bachelorstudium im Fach „Klinische Medizin" an der Südöstlichen Universität**			
09. 2014	**07. 2016**	**Masterstudium im Fach „Klinische Medizin" an der Südöstlichen Universität**			
12. 2016	**jetzt**	**Studium im Heeren Labor an der Hamburg Universität**			
Berufserfahrungen					
06. 2012	**07. 2012**	**Praktikantin im Zentralen Krankenhaus, Stadt Xuzhou, Provinz Jiangsu**			
06. 2013	**06. 2014**	**Praktikum im Generalkrankenhaus Nanjing im Militärbezirk Nanjing**			
06. 2014	**07. 2016**	**Rotation in der Abteilung der inneren Medizin des Gulou-Krankenhaus in Nanjing**			
12.2016	**01.2017**	**Studium an der Hamburg Universität**			

Sprach- und Computerfähigkeit	
Sprachen	**Chinesisch: (Muttersprache)** **Englisch: IELTS-6,0** **Deutsch: B1**
Computer	**Microsoft Office wie word, powerpoint, excel und statistische Softwares wie SPSS und Graphpad geschickt verwenden.**

12. EIDESSTATTLICHE VERSICHERUNG

Ich versichere ausdrücklich, dass ich die Arbeit selbständig und ohne fremde Hilfe verfasst, andere als die von mir angegebenen Quellen und Hilfsmittel nicht benutzt und die aus den benutzten Werken wörtlich oder inhaltlich entnommenen Stellen einzeln nach Ausgabe (Auflage und Jahr des Erscheinens), Band und Seite des benutzten Werkes kenntlich gemacht habe.

Ferner versichere ich, dass ich die Dissertation bisher nicht einem Fachvertreter an einer anderen Hochschule zur Überprüfung vorgelegt oder mich anderweitig um Zulassung zur Promotion beworben habe.

Ich erkläre mich einverstanden, dass meine Dissertation vom Dekanat der Medizinischen Fakultät mit einer gängigen Software zur Erkennung von Plagiaten überprüft werden kann.

Unterschrift: ....